

NATIONAL ADVISORY COMMITTEE FOR AERONAUTICS

TECHNICAL NOTE 2881

AERODYNAMIC CHARACTERISTICS OF A TWO-BLADE

NACA 10-(3)(062)-045 PROPELLER AND OF

A TWO-BLADE NACA 10-(3)(08)-045

PROPELLER

By William Solomon

Langley Aeronautical Laboratory
Langley Field, Va.



Washington

January 1953

TECHNICAL NOTE 2881

AERODYNAMIC CHARACTERISTICS OF A TWO-BLADE

NACA 10-(3)(062)-045 PROPELLER AND OF

A TWO-BLADE NACA 10-(3)(08)-045

PROPELLER¹

By William Solomon

SUMMARY

As part of the investigation to determine the influence of blade-section thickness ratio on propeller performance, tests were made in the Langley 16-foot high-speed tunnel to determine the aerodynamic characteristics of the two-blade NACA 10-(3)(062)-045 propeller and of the two-blade NACA 10-(3)(08)-045 propeller.

Data were obtained over a blade-angle range from 20° to 55° as measured at the 0.75-radius station, the various constant values of rotational speed used giving a range of advance ratio from 0.5 to 3.8. Maximum efficiencies of the order of 91.5 to 92 percent were obtained for the propellers. The propeller with the thinner airfoil sections over the outboard portion of the blades, the NACA 10-(3)(062)-045 propeller, had lower losses at high tip speeds, the difference amounting to about 5 percent at a helical tip Mach number of 1.10.

INTRODUCTION

The aerodynamic characteristics of a series of 10-foot-diameter propellers were investigated in the Langley 16-foot high-speed tunnel in a comprehensive propeller research program. Having high-critical-speed NACA 16-series airfoil sections (ref. 1), these propellers were designed to have Betz minimum induced-energy-loss loading (ref. 2) for a blade angle of 45° at the 0.7 radius when used as a four-blade propeller operating at an advance ratio of approximately 2.1. The ultimate purpose of the program was to determine the influence upon propeller

¹Supersedes the recently declassified NACA RM L8E26, "Aerodynamic Characteristics at High Speeds of a Two-Blade NACA 10-(3)(062)-045 Propeller and of a Two-Blade NACA 10-(3)(08)-045 Propeller" by William Solomon, 1948.

performance of propeller design factors and of compressibility; the propeller tests reported herein form part of the investigation of the effects of blade-section thickness ratio.

SYMBOLS

b	blade width, ft
c_{l_d}	blade-section design lift coefficient
C_P	power coefficient, $P/\rho n^3 D^5$
C_T	thrust coefficient, $T/\rho n^2 D^4$
D	propeller diameter, ft
h	blade-section maximum thickness, ft
J	propeller advance ratio, V/nD
M	air-stream Mach number
M_t	helical tip Mach number, $M \sqrt{1 + \left(\frac{\pi}{J}\right)^2}$
n	propeller rotational speed, rps
P	power absorbed by the propeller, ft-lb/sec
r	radius to a blade element, ft
R	propeller tip radius, ft
T	propeller thrust, lb
V	airspeed, fps
β	blade angle, deg
$\beta_{0.75R}$	blade angle at 0.75 tip radius, deg
η	propeller efficiency, $\frac{C_T}{C_P} J$

η_i optimum efficiency (zero profile-drag losses)

ρ mass density of air, slugs/cu ft

APPARATUS

Propeller dynamometer. - A diagram showing the configuration for these propeller tests with the 2000-horsepower dynamometer is shown in figure 1. The test apparatus and thrust and torque measuring devices are described in detail in reference 3.

Propeller blades. - The blades are of NACA 10-(3)(062)-045 and NACA 10-(3)(08)-045 design which have designation numbers descriptive of the propeller shape, size, and design aerodynamic characteristics. The numerals of the first group give the diameter in feet; the numerals within the first parentheses give the design lift coefficient, in tenths, of the blade section at the 0.7 radius; the numerals within the second parentheses give the thickness ratio at the 0.7 radius; and the last group designates the solidity of one blade of the propeller at the 0.7 radius. Solidity is the ratio of the blade width at any radius to the circumference of the circle traversed by that blade section. Blade-form curves for these propellers are shown in figure 2. As can be seen, the blades differ only in thickness ratio and, very slightly, in blade angle; blade-width ratio and design lift coefficient are identical for the two propellers. A photograph of typical propeller blades mounted on the propeller dynamometer in the tunnel is shown as figure 3. Efficient airfoil sections extend to the spinner of the two-blade test propeller. Spinner fairing plates with 0.062-inch clearance between blade and spinner were provided for each blade angle tested.

TEST PROCEDURE

Tests of the propellers were made at blade angles varying in 5° increments from 20° to 55° at the 0.75 radius (45-in. radius). Most tests were run at constant rotational speed, the range of advance ratio ($J = V/nD$) being obtained by changing the tunnel airspeed. A chart of the various rotational speeds giving the blade angles tested at each speed is given as table I. Because of power limitations, tests could not be made at high blade angle and high rotational speed. Therefore, in order to obtain propeller characteristics over a greater range of tip Mach number, tests were run at a blade angle of 45° for maximum dynamometer power and airspeed at or near maximum tunnel airspeed. For these tests the tunnel airspeed was kept constant and the dynamometer rotational speed was varied to obtain the range of advance ratio required.

RESULTS AND DISCUSSION

Reduction of data. - The test data, corrected for spinner force and tunnel-wall interference, are presented as the usual propeller characteristics, thrust and power coefficient and propeller efficiency plotted as functions of advance ratio. Reference 3 describes the corrections applied. Propeller characteristics as presented herein represent the forces exerted by the propeller from the spinner surface to the blade tips acting in free air. These data are believed to be accurate to within 1 percent.

Because the tests were made over a period of time (therefore, under different conditions of tunnel air temperature), small discontinuities occurred in the curves of air-stream Mach number plotted against advance ratio. Also, discrepancies occurred between the values of stream Mach number at the same value of advance ratio for tests run at different times. Therefore, in order to obtain uniformity in the presented data, all air-stream Mach number curves and helical tip Mach number curves have been corrected to those presented for the same advance ratio and rotational speed for the basic propeller of the NACA series, the NACA 10-(3)(08)-03 propeller, in reference 3.

Propeller characteristics. - Fairied curves of thrust coefficient, power coefficient, and propeller efficiency plotted as functions of advance ratio are presented in figures 4 to 10 for the two-blade NACA 10-(3)(062)-045 propeller and in figures 11 to 17 for the two-blade NACA 10-(3)(08)-045 propeller. The variation of air-stream Mach number and helical tip Mach number with advance ratio is shown in the figures presenting propeller efficiency.

Envelope efficiency. - Envelope curves of propeller efficiency at the various test rotational speeds are given for the two-blade NACA 10-(3)(062)-045 propeller in figure 18 and for the two-blade NACA 10-(3)(08)-045 propeller in figure 19. Also shown in these figures is the optimum efficiency η_i of a two-blade propeller with Betz minimum induced-energy-loss loading operating at 1350 rpm. The optimum-efficiency curve was calculated by a method, given in reference 4, which neglects all profile-drag losses for a two-blade propeller operating at the same values of power coefficient as attained in the tests of the NACA propellers. At the higher values of advance ratio, 2.0 to 2.8, the calculated values of optimum efficiency are higher for the NACA 10-(3)(062)-045 propeller than for the NACA 10-(3)(08)-045 propeller because the thinner propeller operates at slightly lower values of power coefficient for maximum efficiency than does the thicker propeller. This higher optimum-efficiency value for the NACA 10-(3)(062)-045 propeller is in agreement with propeller theory which indicates that at

maximum efficiency the blade-section profile-drag losses should approximately equal the induced losses; therefore, the propeller with the lower profile-drag loss, the propeller with thinner blade sections, will operate under lighter load and, consequently, with lower induced loss.

Comparison of this optimum-efficiency curve with the envelope efficiency curve (1350 rpm) for both propellers indicates induced losses of the order of 5 percent and profile-drag losses of the order of 4 percent at an advance ratio of 2.2, approximately the design advance ratio. The high peak of the envelope efficiency curve (91.5 to 92 percent) is a result of the use of a Betz loading in the design and the maintaining of efficient airfoil sections to the spinner surface.

Comparison of NACA 10-(3)(08)-045 data with NACA 4-(3)(08)-045 data. The envelope efficiency of the two-blade NACA 10-(3)(08)-045 propeller at 1350 rpm is compared in figure 20 with corresponding results from tests of a 4-foot-diameter model of this propeller (ref. 5). Also shown in the figure are the optimum-efficiency curves for the values of power coefficient at maximum efficiency obtained with the respective propellers. Since, during the tests of the 4-foot-diameter propeller, the propeller was mounted on the forward portion of a model with a wing spanning the tunnel and since thrust was measured by the tunnel balance system, some of the slipstream rotation was converted into measured thrust. Therefore, the propulsive efficiencies which were obtained considerably exceeded the propeller efficiencies obtained with the 10-foot-diameter propeller. Also, for the 4-foot-diameter propeller, the peak values of efficiency occurred at higher values of advance ratio and, consequently, at lower values of power coefficient. Hence, the values of optimum efficiency for the 4-foot-diameter propeller are higher than optimum-efficiency values for the 10-foot-diameter propeller. In an analysis made in England by A. B. Haines shortly after publication of reference 5, comments were presented to point out an apparent discrepancy, as follows: envelope efficiency for the model propeller (NACA 4-(3)(08)-045) approached optimum propeller efficiency with increasing advance ratio and then equaled the optimum at the higher values of advance ratio. This discrepancy exists only if the envelope efficiency for the 4-foot-diameter propeller is compared with optimum efficiency calculated from excessively high values of power coefficient.

At low advance ratio where small amounts of rotational energy are imparted to the slipstream, the effect of the wing on recovery of the energy in the form of thrust is very small. At higher blade angles and advance ratios, where relatively much larger amounts of rotational energy are imparted to the slipstream, a significant increment of thrust is obtained from the partial recovery of the rotational energy by the wing. Calculations based on the method of reference 6 show that at high advance ratios the wing recovers approximately 50 percent of the slipstream rotational energy in the form of thrust; this amounts to approximately 2 percent in efficiency. Therefore, a major part of the total

difference between the results of the 4-foot and the 10-foot-diameter-propeller tests is accounted for by this one factor.

Compressibility effects. - The maximum efficiency of the two-blade NACA 10-(3)(08)-045 and the two-blade NACA 10-(3)(062)-045 propellers at a blade angle of 45° is shown in figure 21 for a range of helical tip Mach number. At the lower tip Mach numbers there is little difference between the maximum efficiency of the propellers. Above a tip Mach number of 0.90, the maximum efficiency of both propellers decreases rapidly. However, the rate of this maximum-efficiency decrease is lower for the propeller with the thinner outboard blade sections. With an increase of helical tip Mach number from 0.92 to 1.10, the loss in maximum efficiency is 13 percent for the NACA 10-(3)(062)-045 propeller as compared with an 18-percent loss for the NACA 10-(3)(08)-045 propeller, the propeller with the thicker outboard blade sections. The higher efficiency of the propeller with the thinner outboard blade sections is expected because airfoil section data show that thin sections maintain their lift to higher Mach numbers than thick sections (ref. 1).

CONCLUDING REMARKS

An investigation was made in the Langley 16-foot high-speed tunnel to determine the aerodynamic characteristics of the two-blade NACA 10-(3)(062)-045 and the two-blade NACA 10-(3)(08)-045 propellers, differing principally in thickness distribution. Data are presented over a range of advance ratio from 0.5 to 3.8 and a blade-angle range from 20° to 55° measured at the 0.75 radius.

These propellers, as a result of the use of a Betz loading in the design and the maintaining of efficient airfoil sections to the spinner surface, have a maximum efficiency of the order of 91.5 to 92 percent.

The propeller with the thinner airfoil sections over the outboard portion of the blades has lower losses in maximum efficiency caused by compressibility, the difference amounting to about 5 percent at a helical tip Mach number of 1.10.

Langley Aeronautical Laboratory,
National Advisory Committee for Aeronautics,
Langley Field, Va., June 11, 1948.

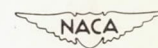
REFERENCES

1. Stack, John: Tests of Airfoils Designed To Delay the Compressibility Burble. NACA Rep. 763, 1943. (Supersedes NACA TN 976.)
2. Hartman, Edwin P., and Feldman, Lewis: Aerodynamic Problems in the Design of Efficient Propellers. NACA WR L-753, 1942. (Formerly NACA ACR, Aug. 1942.)
3. Corson, Blake W., Jr., and Maynard, Julian D.: The Langley 2,000-Horsepower Propeller Dynamometer and Tests at High Speed of an NACA 10-(3)(08)-03 Two-Blade Propeller. NACA TN 2859, 1952. (Supersedes NACA RM L7L29.)
4. Crigler, John L., and Talkin, Herbert W.: Charts for Determining Propeller Efficiency. NACA WR L-144, 1944. (Formerly NACA ACR L4I29.)
5. Stack, John, Draley, Eugene C., Delano, James B., and Feldman, Lewis: Investigation of the NACA 4-(3)(08)-03 and NACA 4-(3)(08)-045 Two-Blade Propellers at Forward Mach Numbers to 0.725 To Determine the Effects of Compressibility and Solidity on Performance. NACA Rep. 999, 1950. (Supersedes NACA ACR's 4A10 and 4B16.)
6. Betz, Albert: The Theory of Contra-Vanes Applied to the Propeller. NACA TM 909, 1939.

TABLE I

RANGE OF BLADE ANGLE AND ROTATIONAL SPEED

Figure	Rotational speed, rpm	β at 0.75R, deg								
NACA 10-(3)(062)-045 propeller										
4	1140		25	30	35	40	45		50	55
5	1350	20	25	30	35	40	45		50	
6	1500						45			
7	1600	20	25	30	35	40	45			
8	2000	20	25	30	35					
9	2160	20	25	30						
10	Varied						45			
NACA 10-(3)(08)-045 propeller										
11	1140		30	35	40	45		50	55	
12	1350	20	25	30	35	40	45		50	
13	1500						45			
14	1600	20	25	30	35	40	45			
15	2000	20	25	30	35					
16	2160	20	25	30						
17	Varied						45			



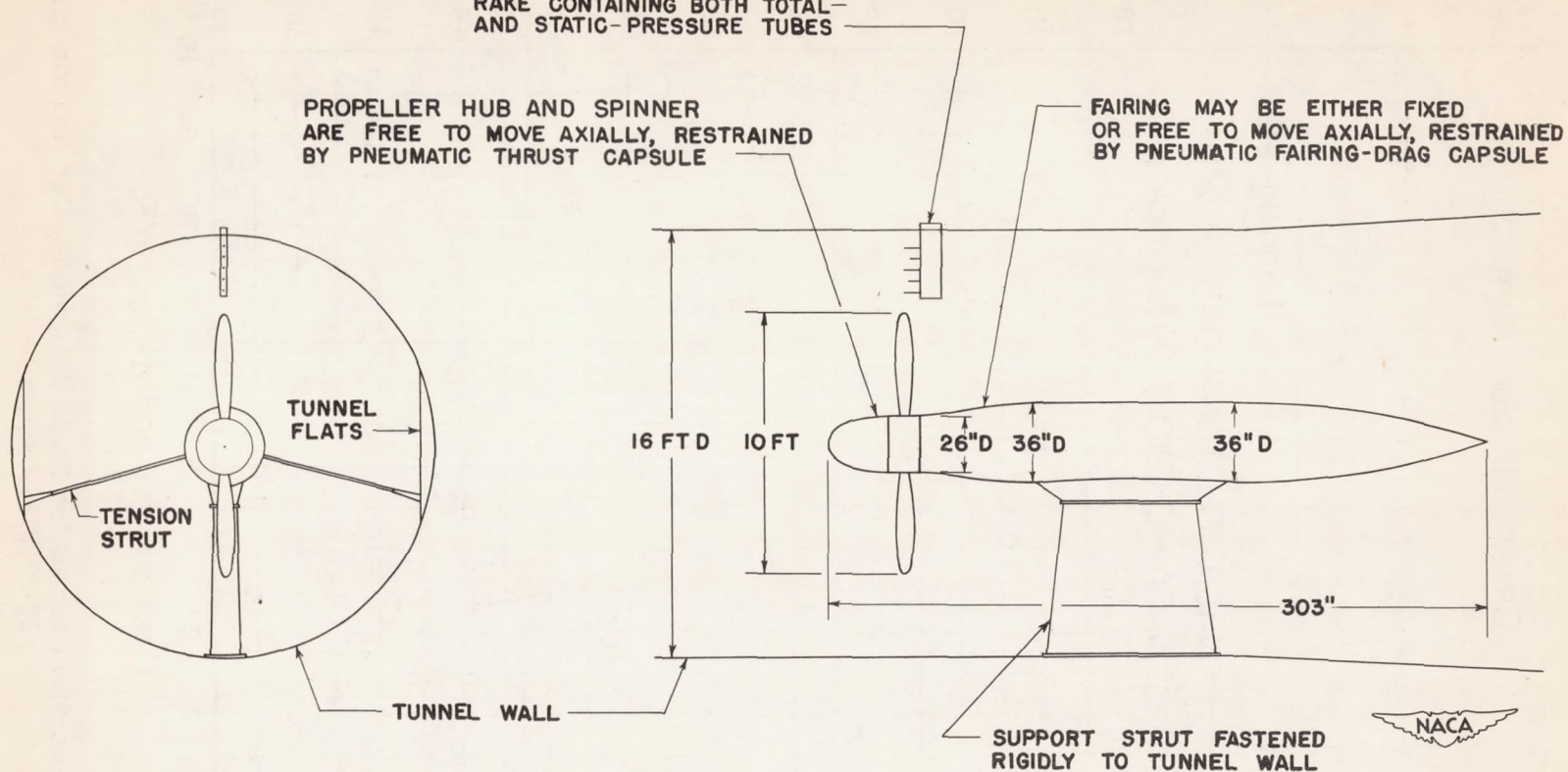


Figure 1.- Configuration of 2000-horsepower dynamometer for tests of propellers in the Langley 16-foot high-speed tunnel.

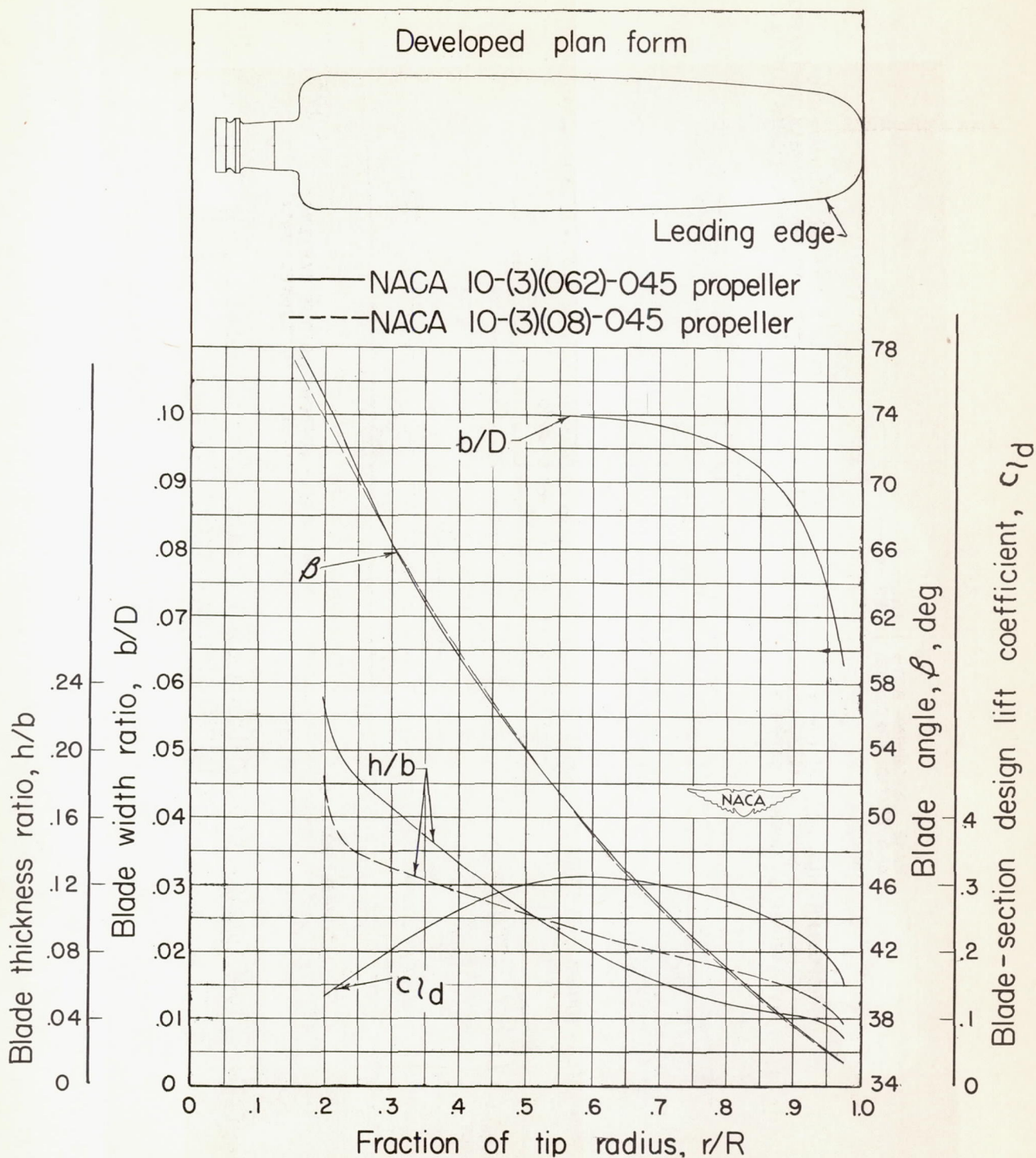


Figure 2.- Blade-form curves for NACA 10-(3)(062)-045 and for NACA 10-(3)(08)-045 propellers.

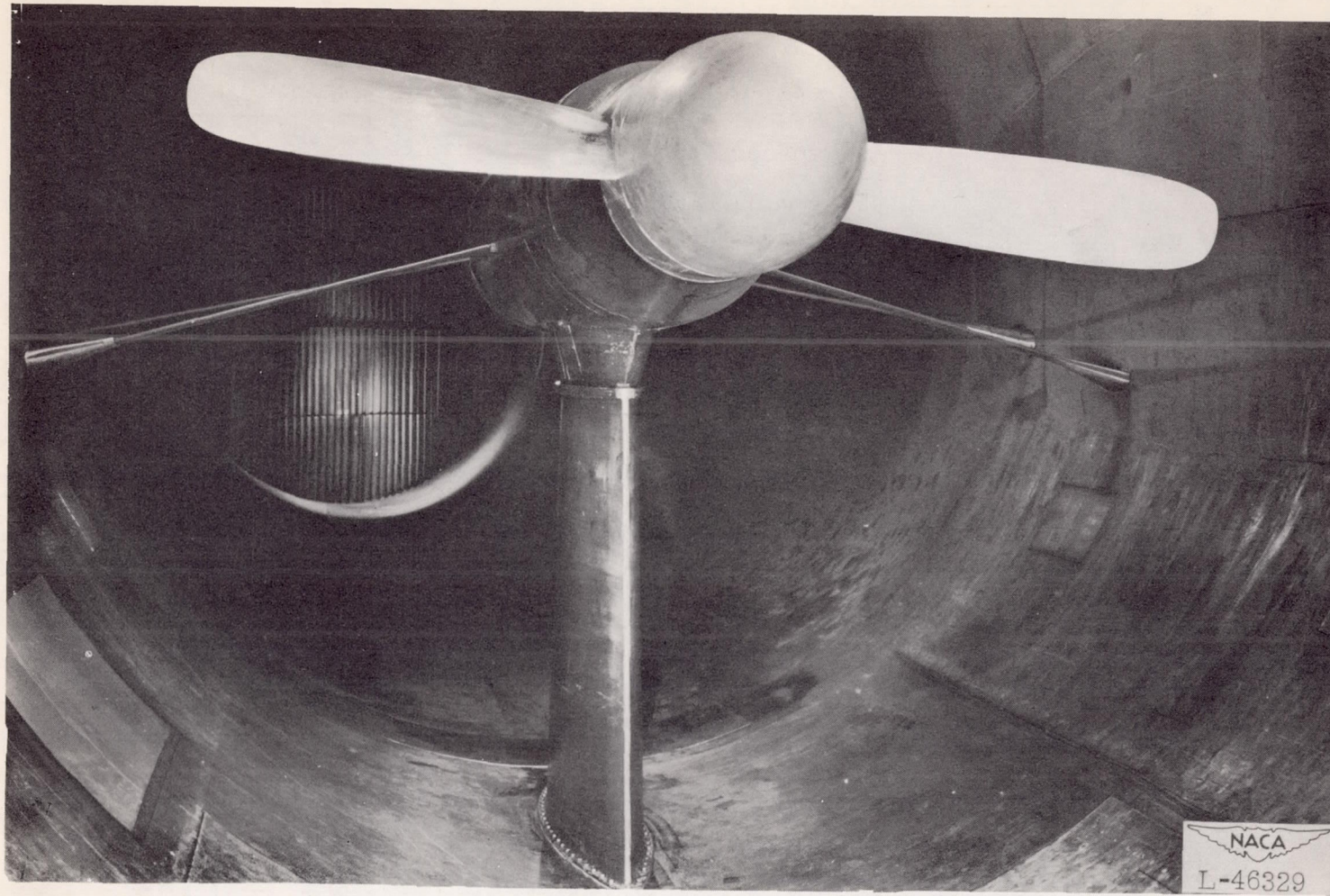
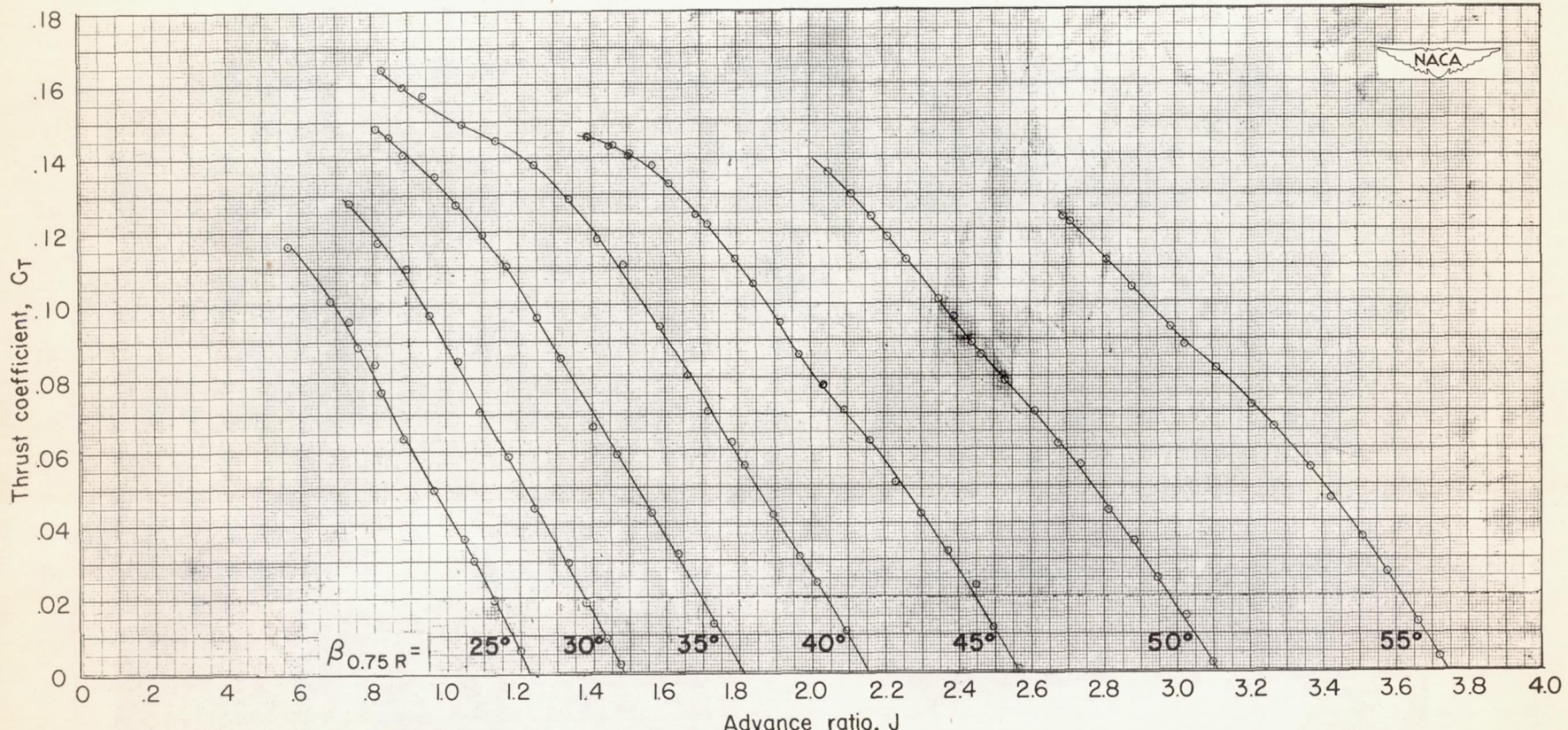
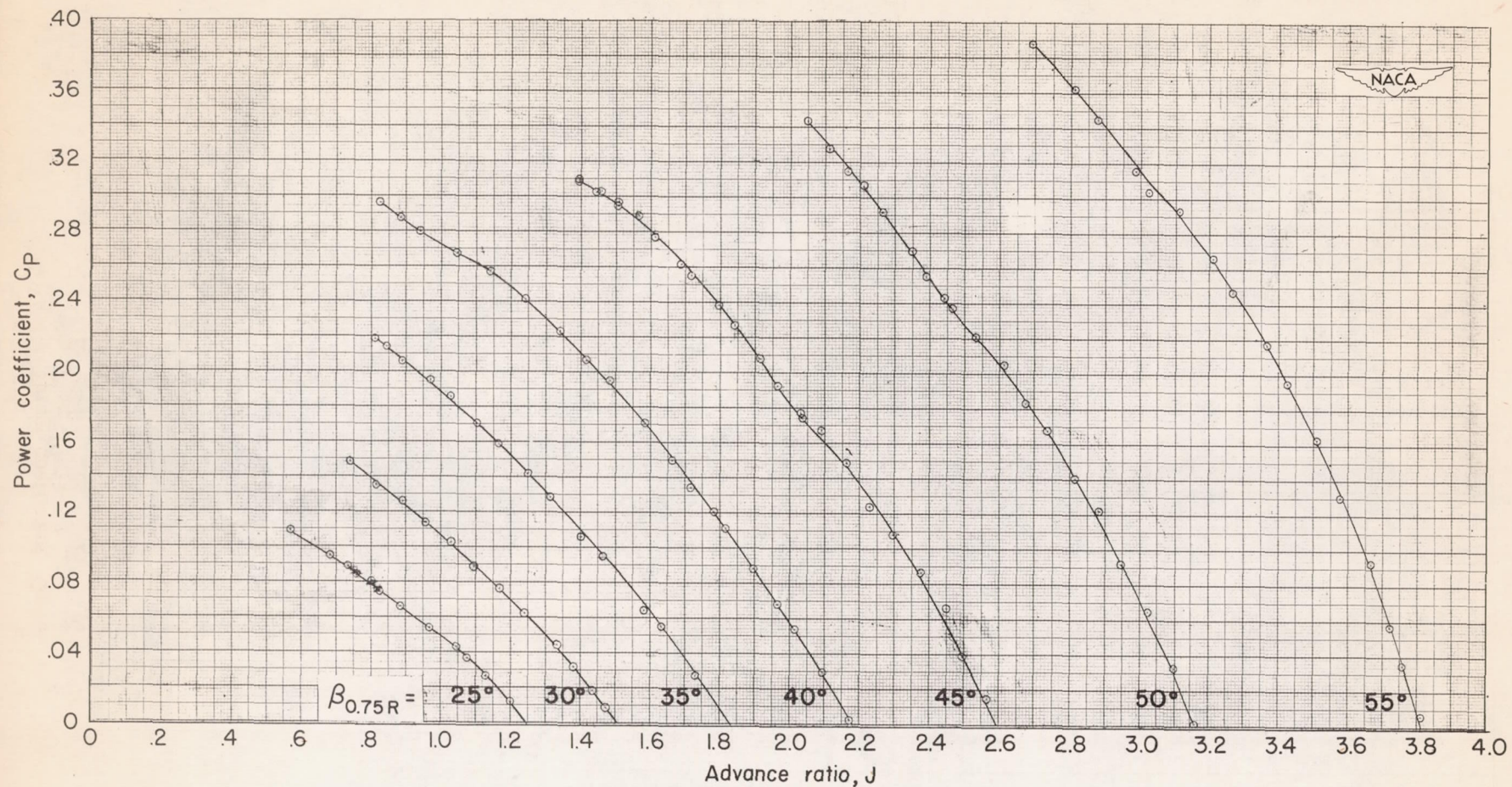


Figure 3.- Typical propeller blade mounted on the propeller dynamometer.



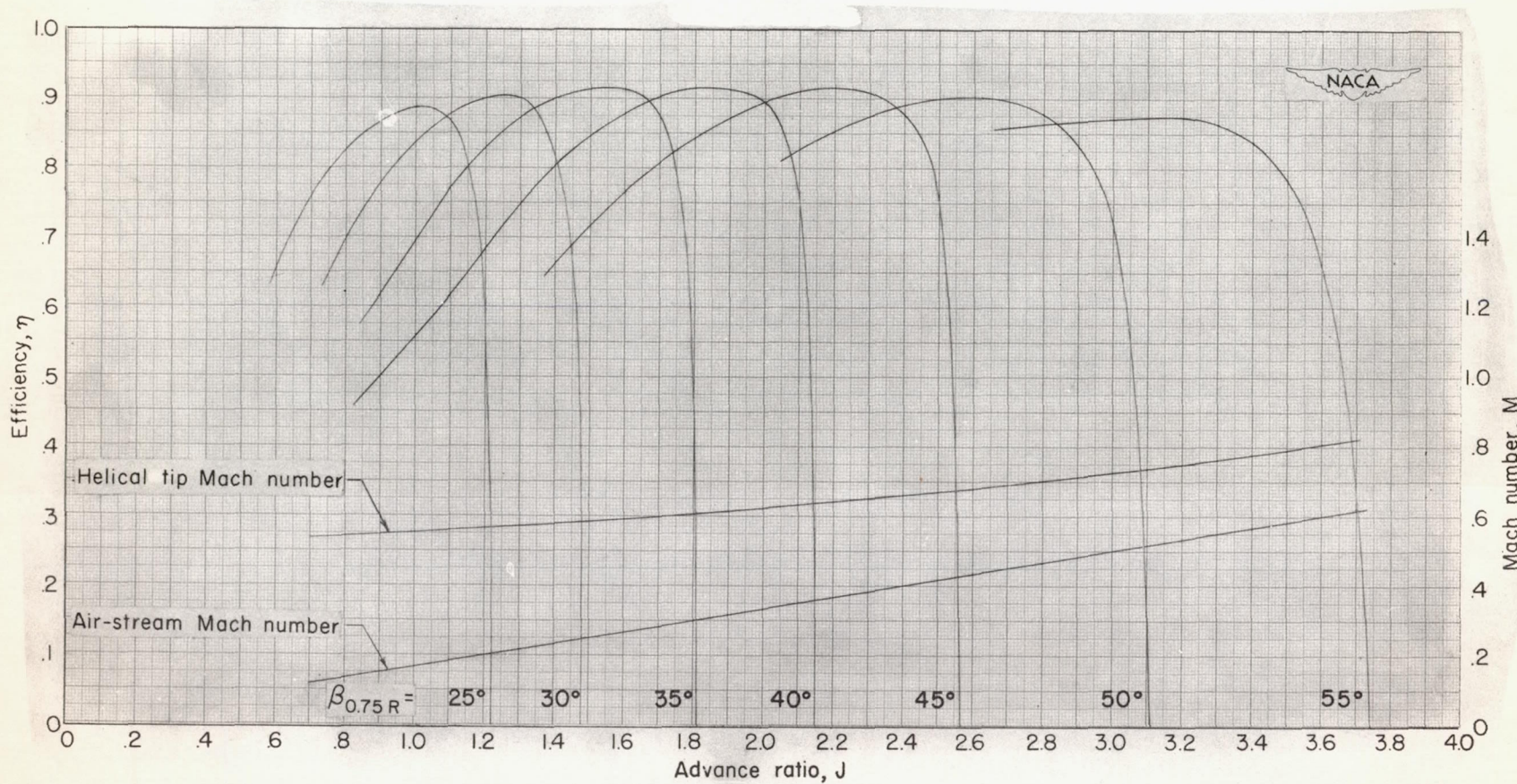
(a) Thrust coefficient.

Figure 4.- Characteristics of two-blade NACA 10-(3)(062)-045 propeller. Rotational speed, 1140 rpm.



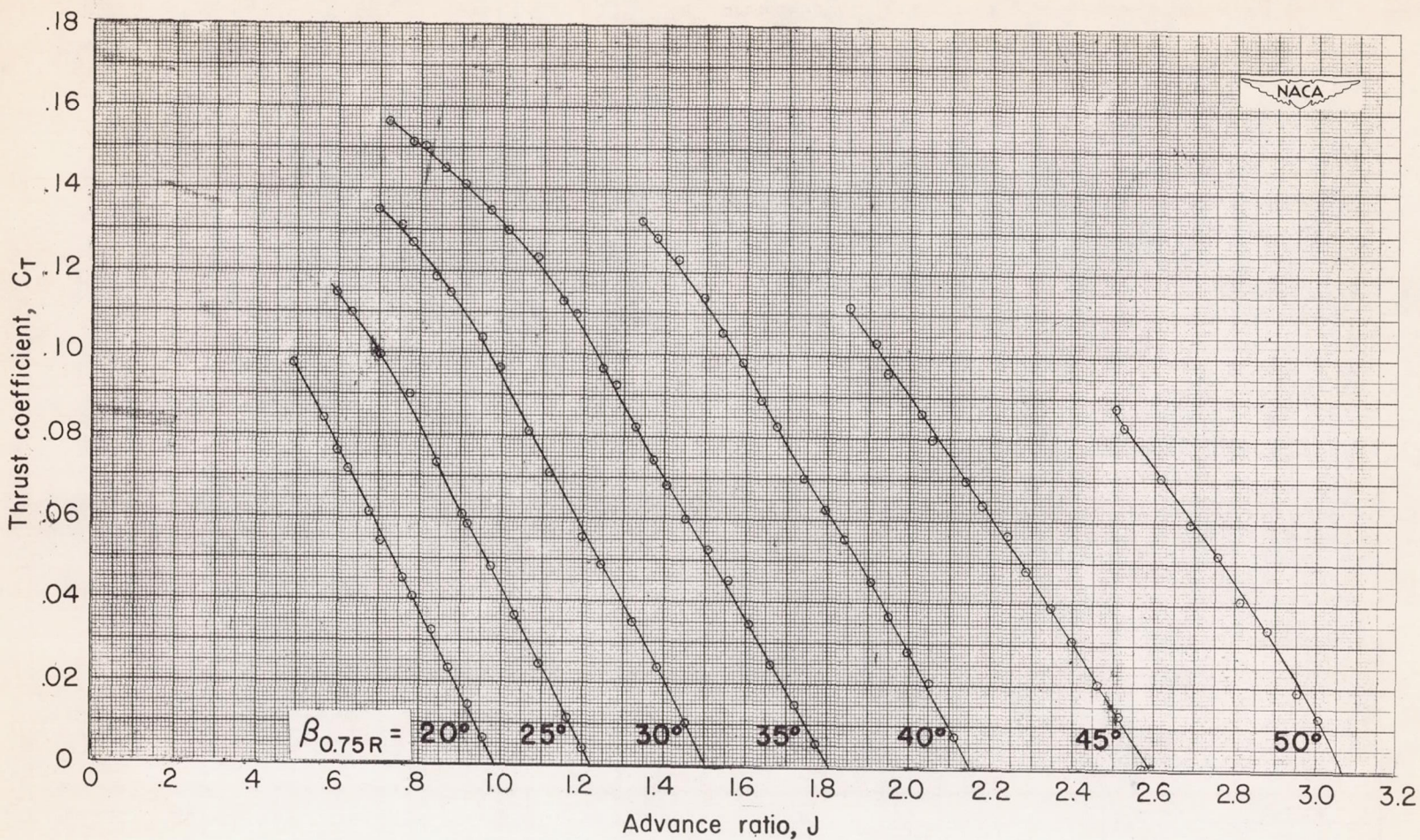
(b) Power coefficient.

Figure 4.- Continued.



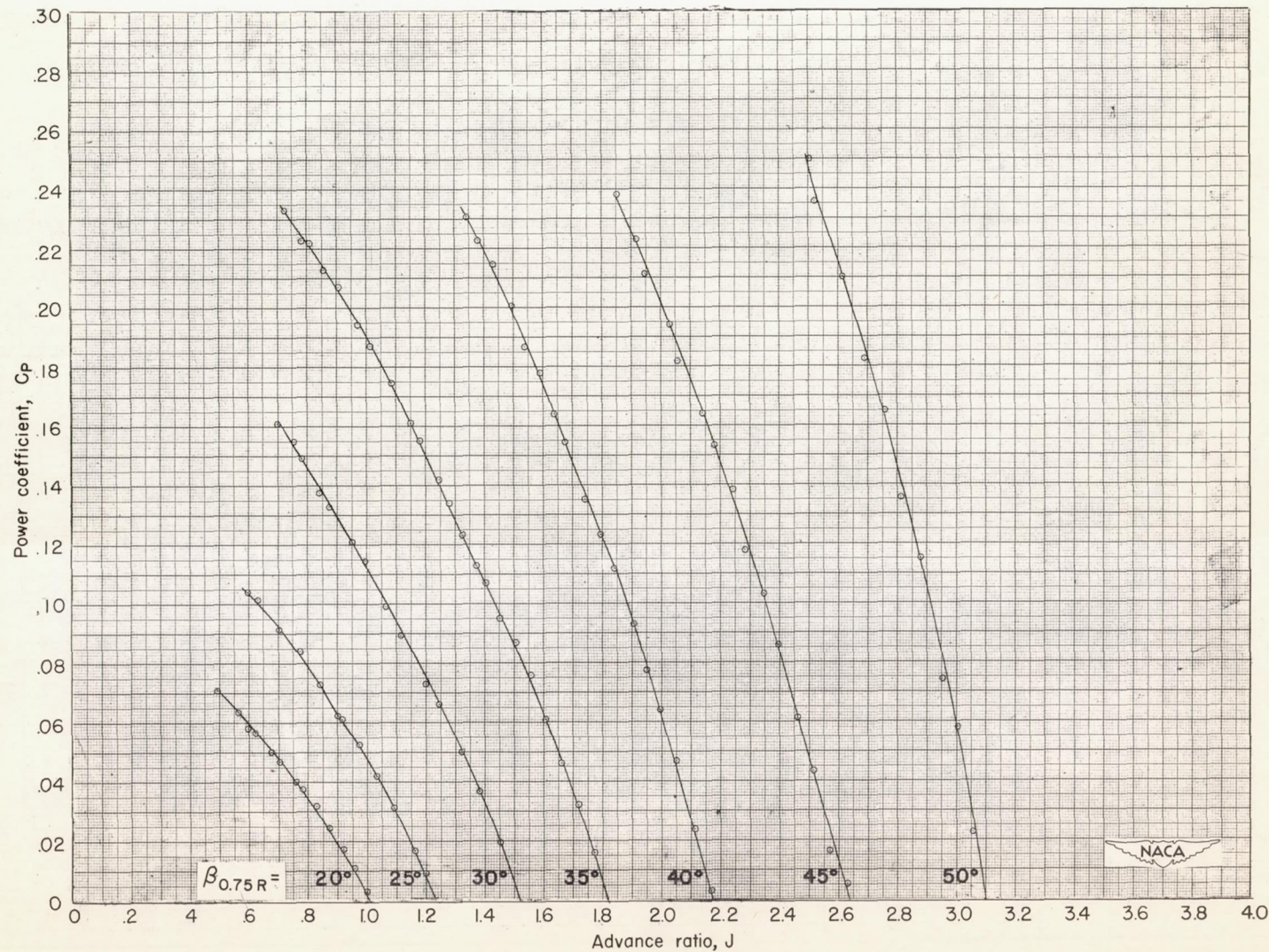
(c) Efficiency.

Figure 4.- Concluded.



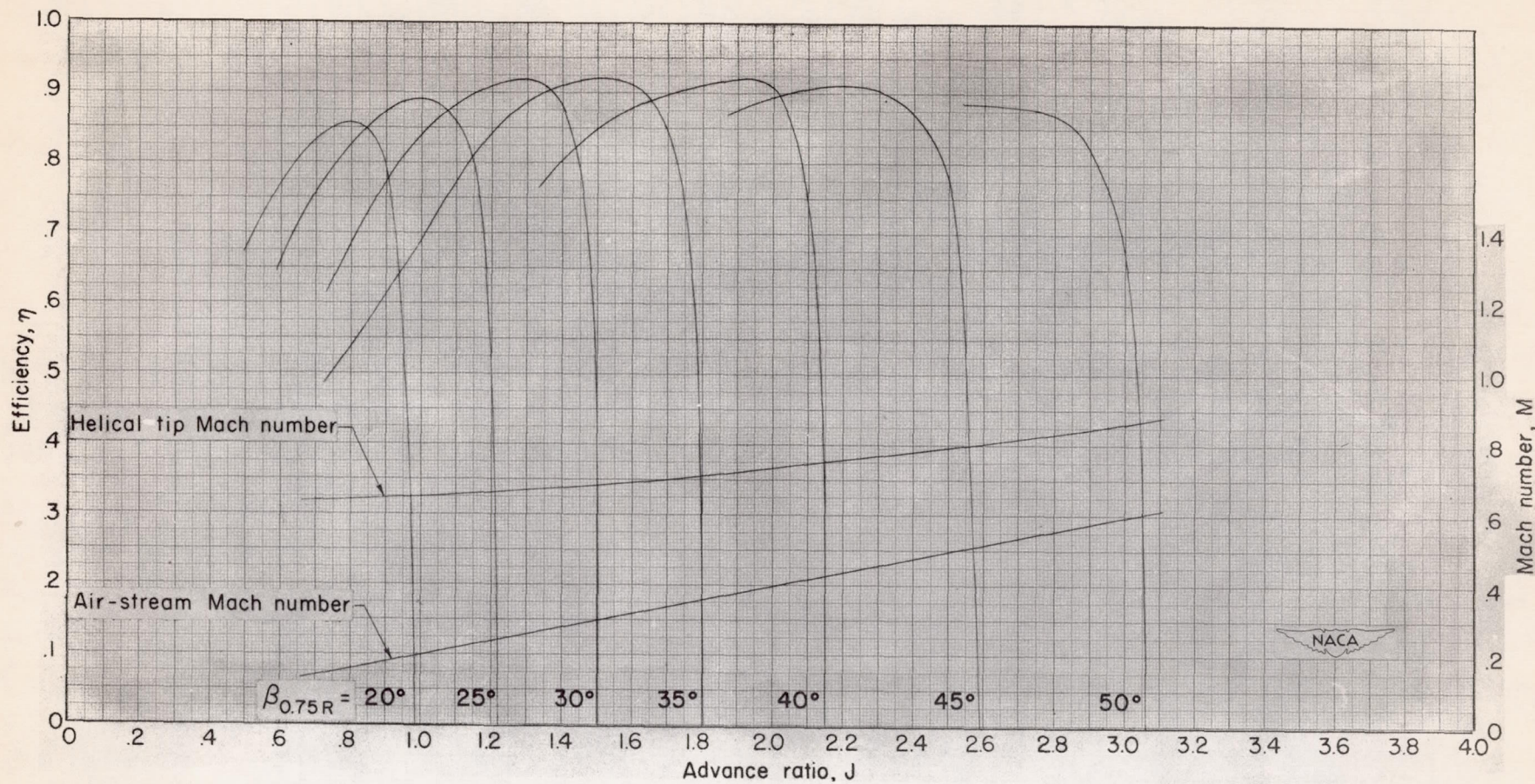
(a) Thrust coefficient.

Figure 5.- Characteristics of two-blade NACA 10-(3)(062)-045 propeller. Rotational speed, 1350 rpm.



(b) Power coefficient.

Figure 5.- Continued.



(c) Efficiency.

Figure 5.- Concluded.

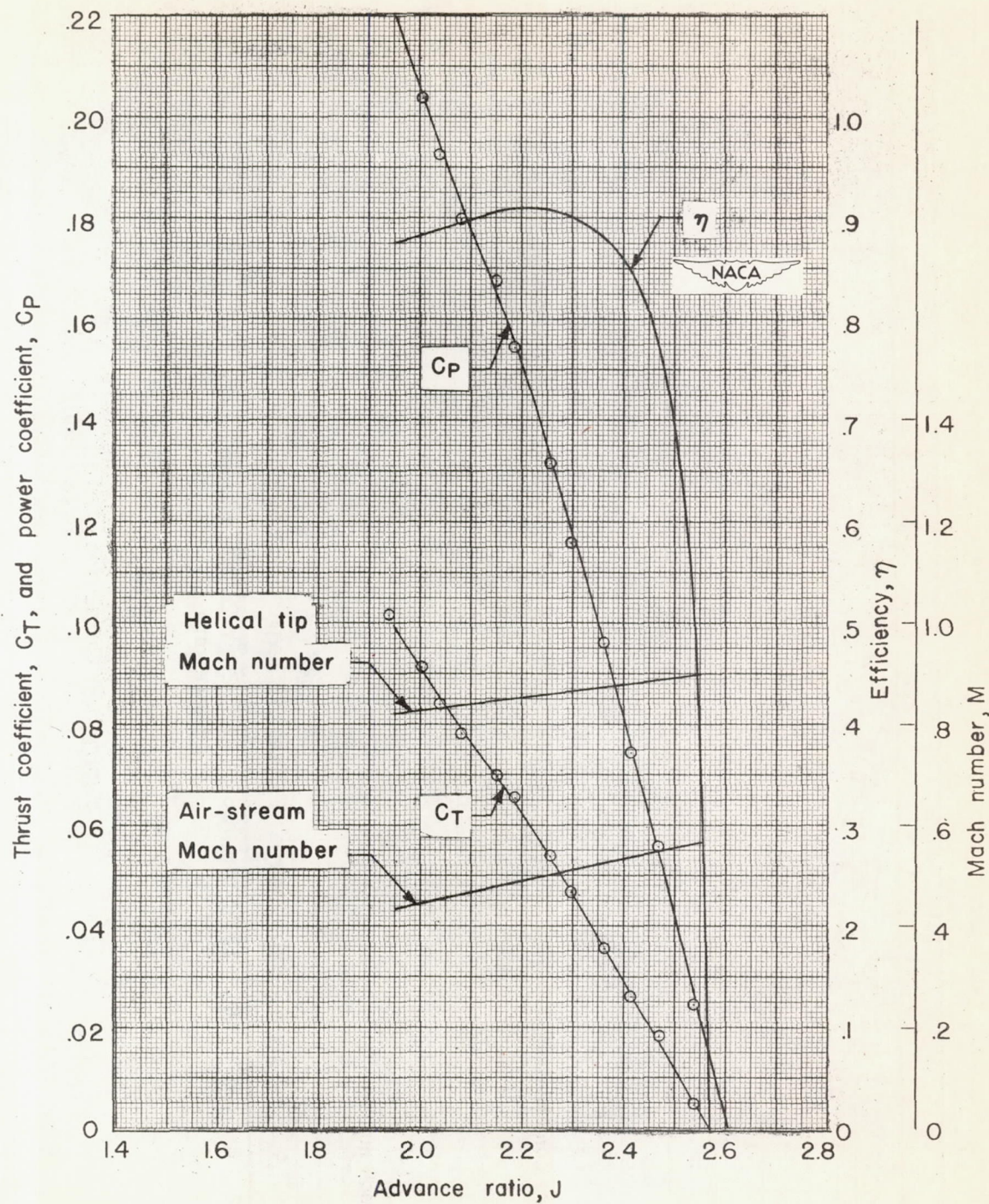
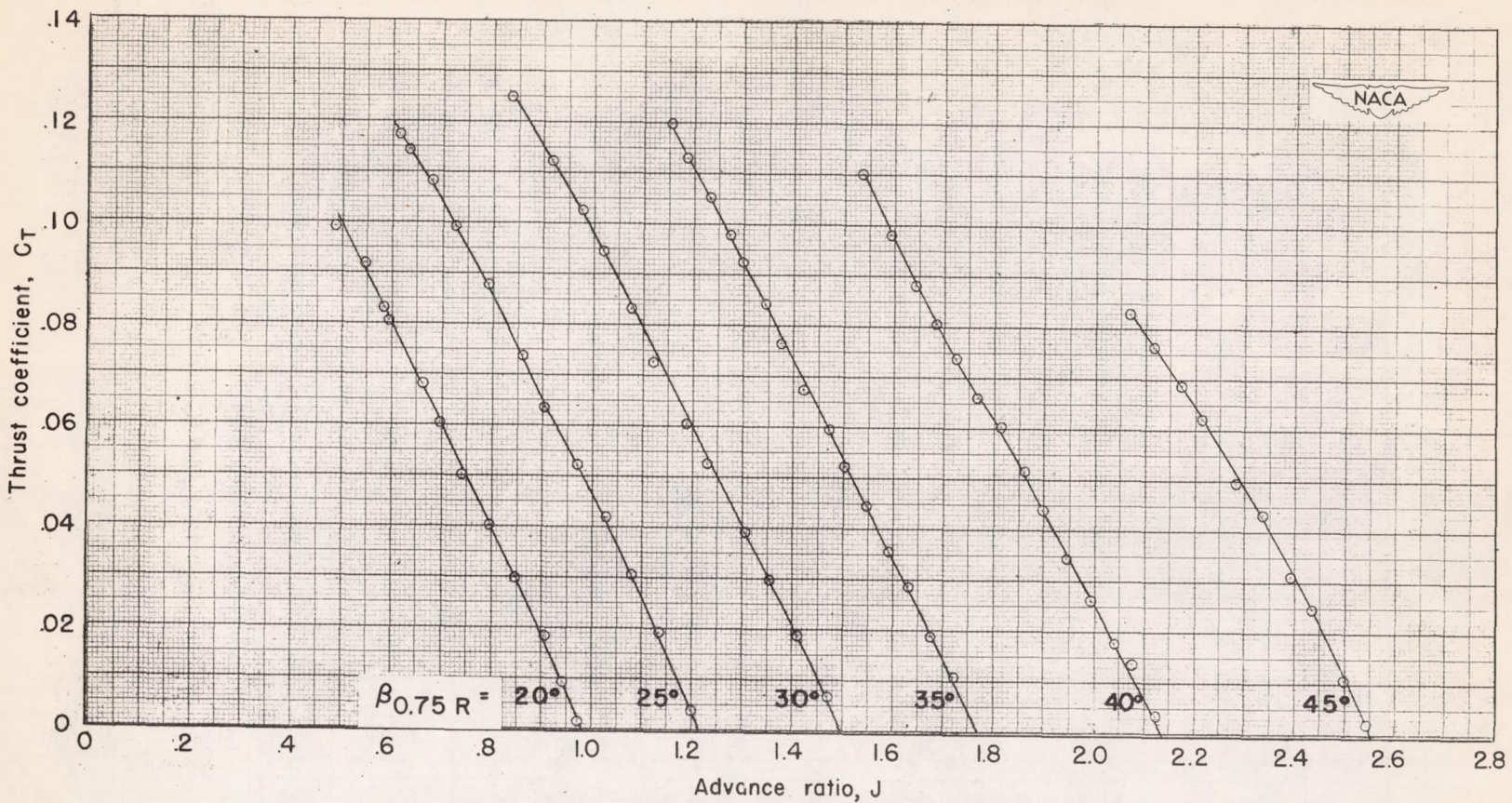
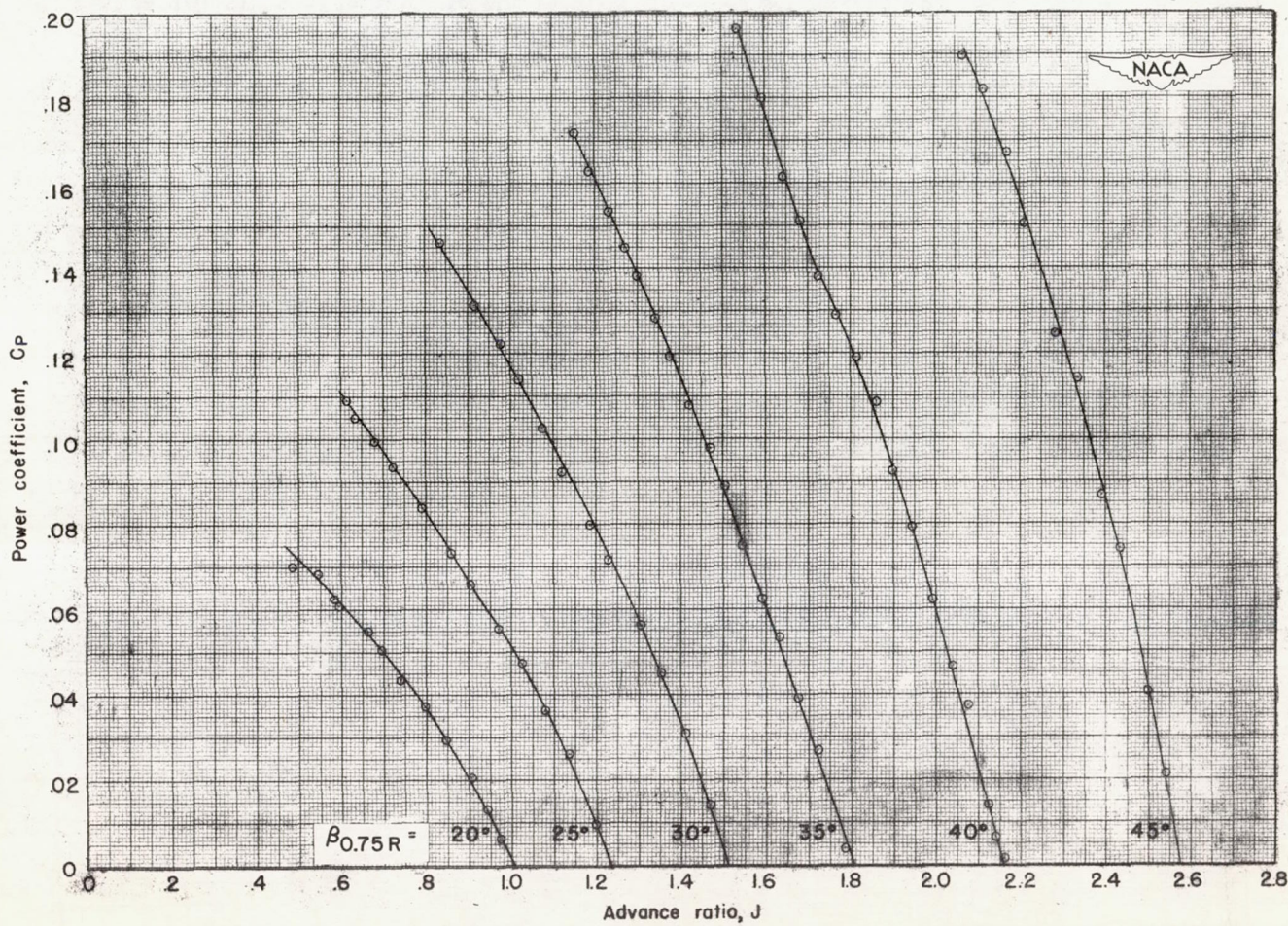


Figure 6.- Characteristics of two-blade NACA 10-(3)(062)-045 propeller.
Rotational speed, 1500 rpm; $\beta_{0.75R} = 45^\circ$.



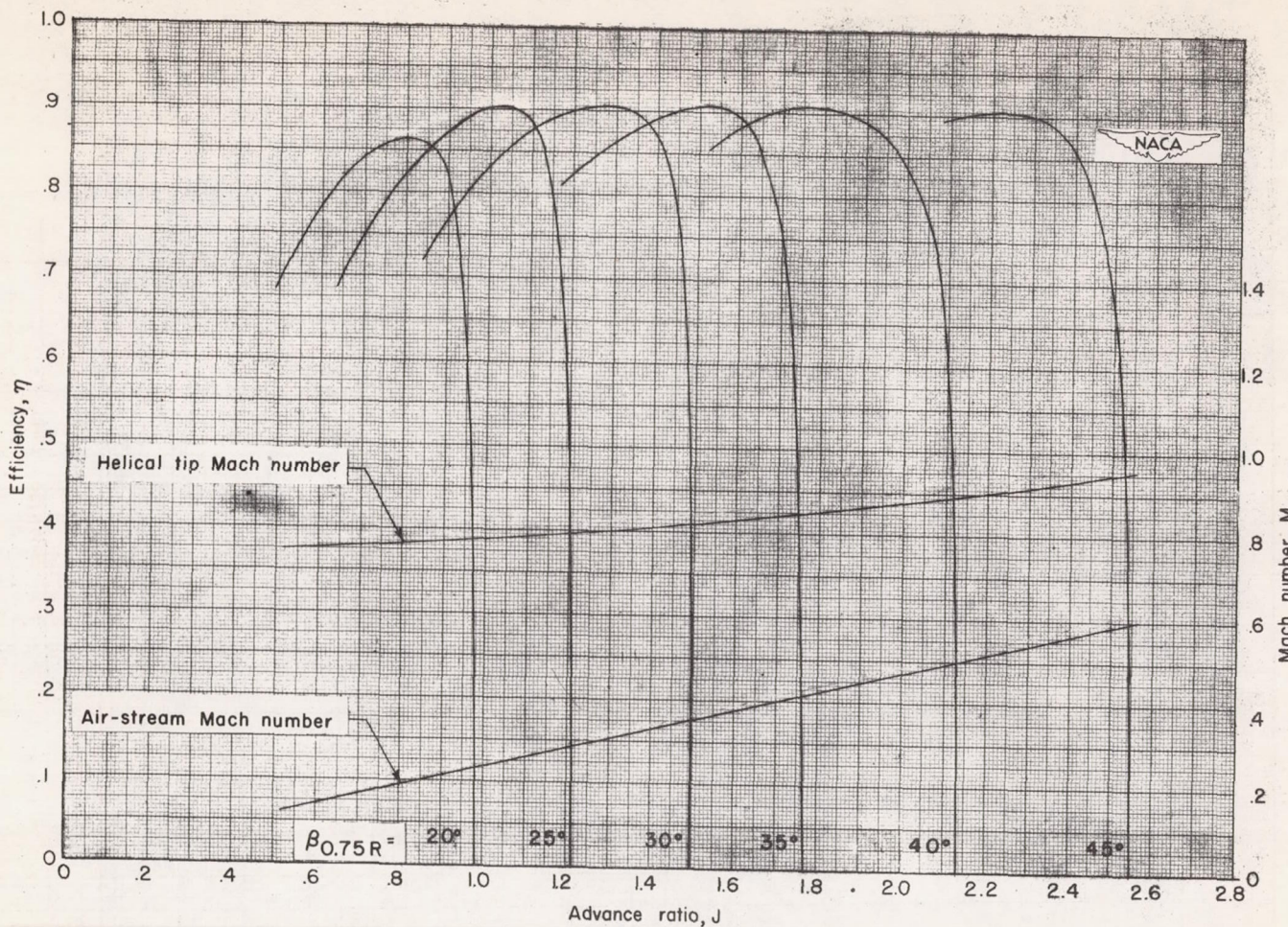
(a) Thrust coefficient.

Figure 7.- Characteristics of two-blade NACA 10-(3)(062)-045 propeller. Rotational speed, 1600 rpm.



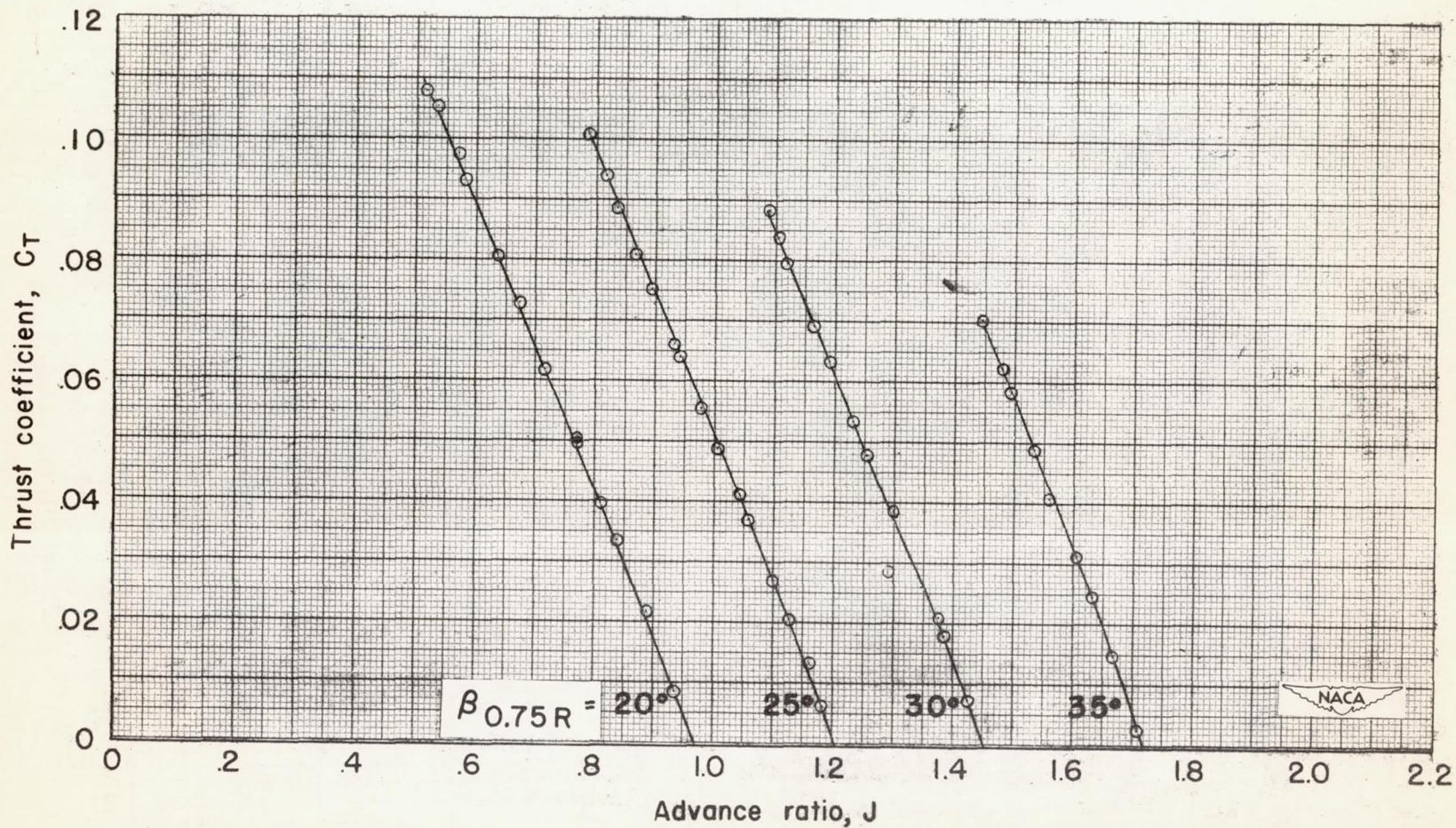
(b) Power coefficient.

Figure 7.- Continued.



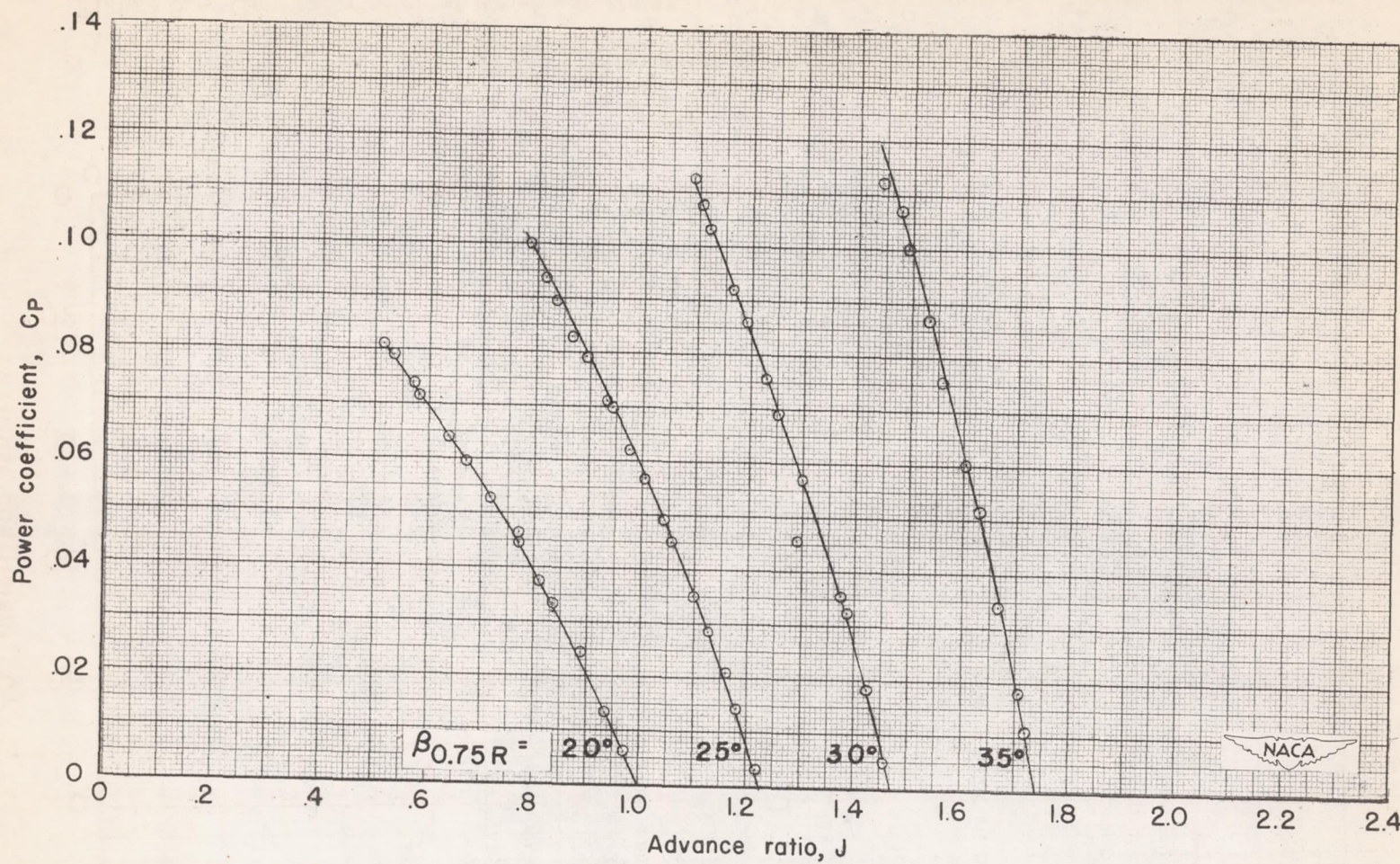
(c) Efficiency.

Figure 7.- Concluded.



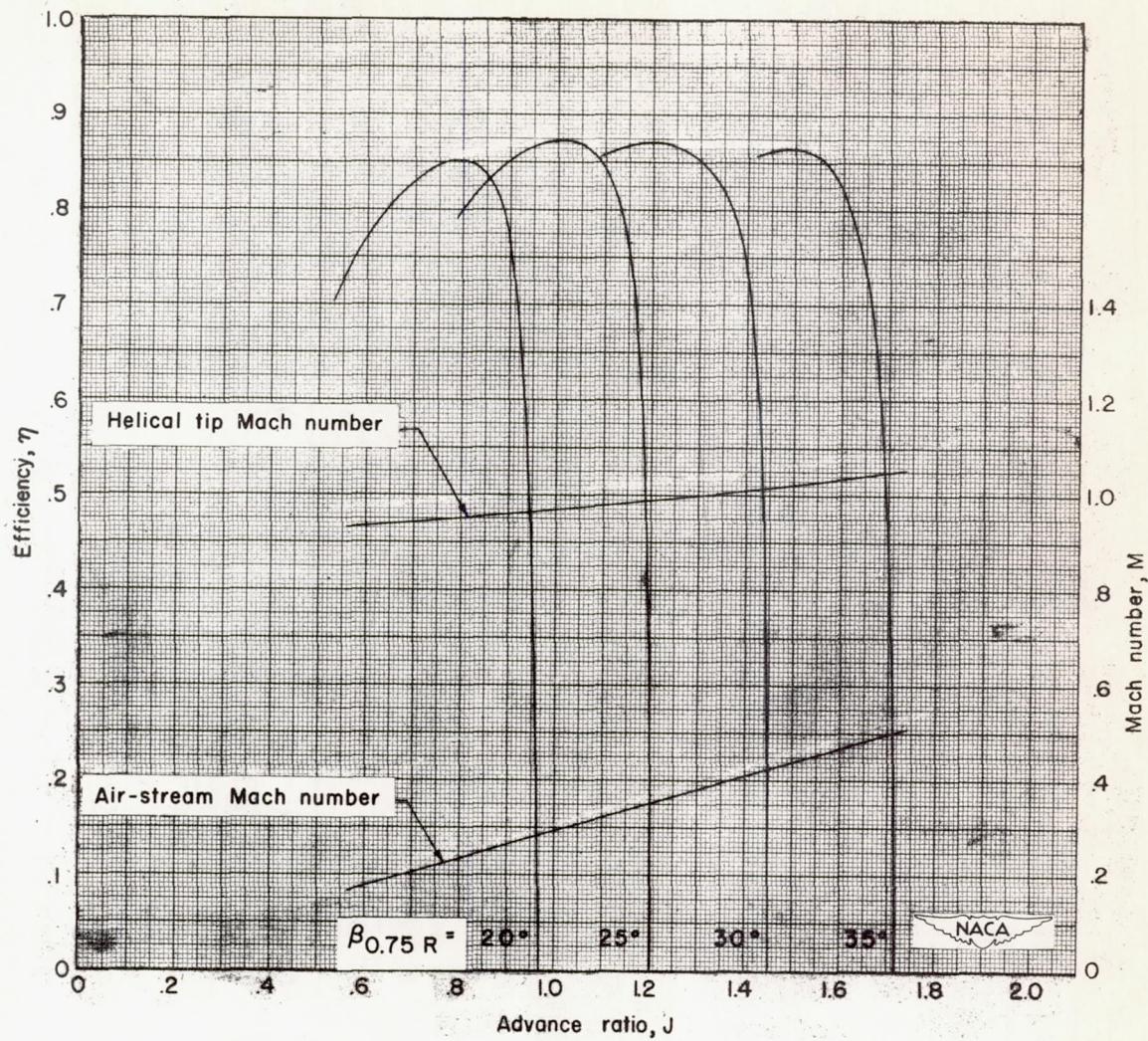
(a) Thrust coefficient.

Figure 8.- Characteristics of two-blade NACA 10-(3)(062)-045 propeller. Rotational speed, 2000 rpm.



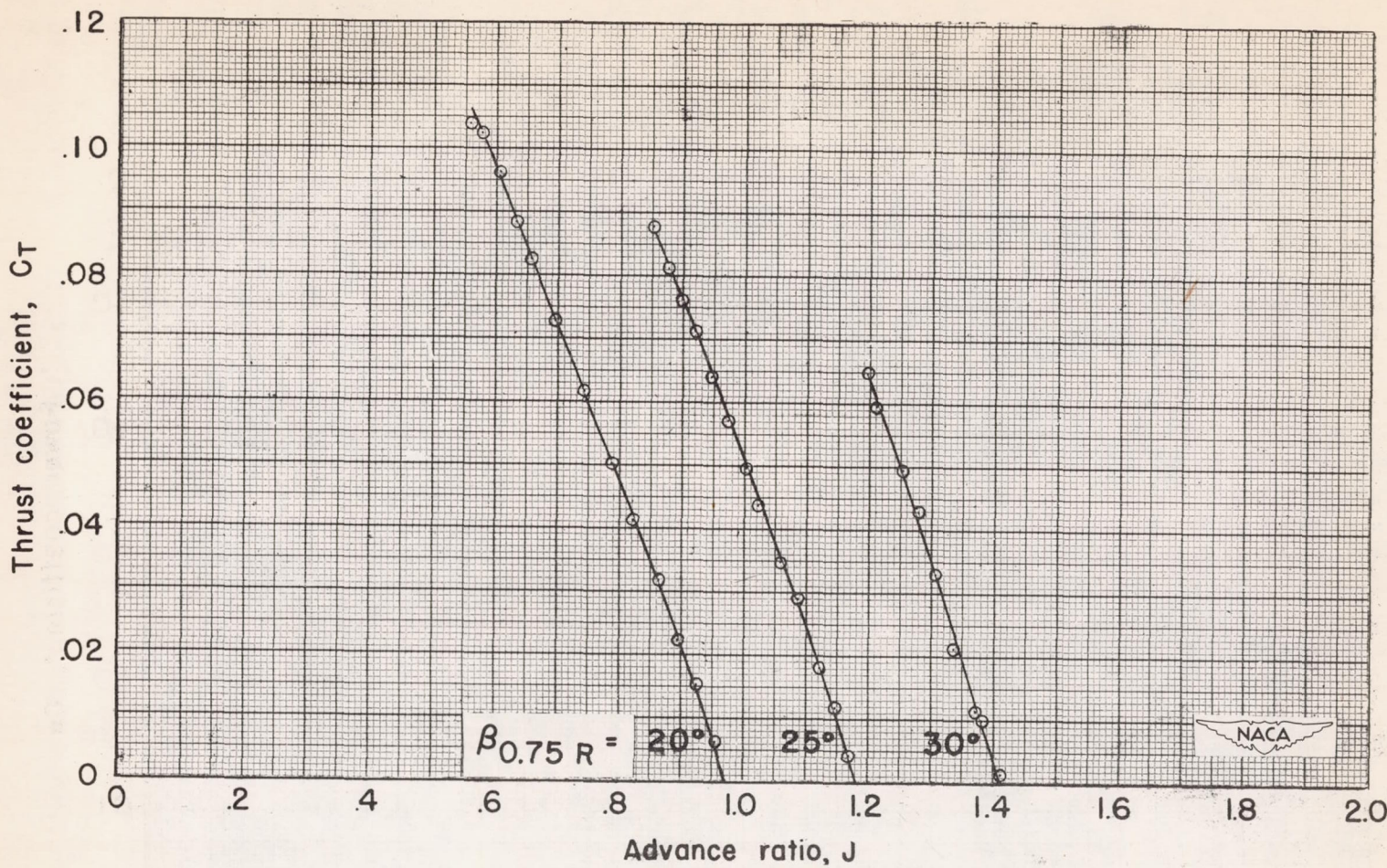
(a) Power coefficient.

Figure 8.- Continued.



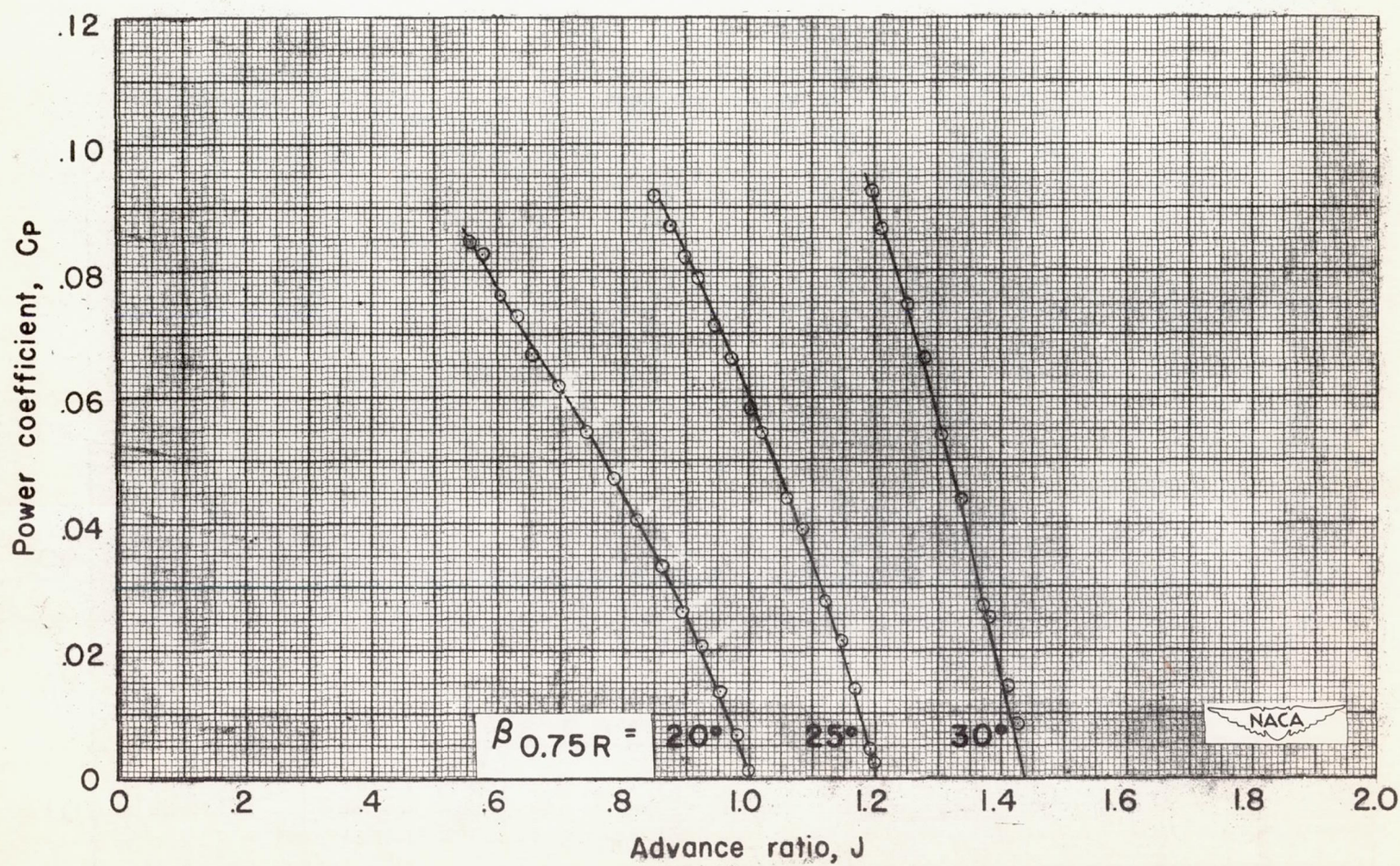
(c) Efficiency.

Figure 8.- Concluded.



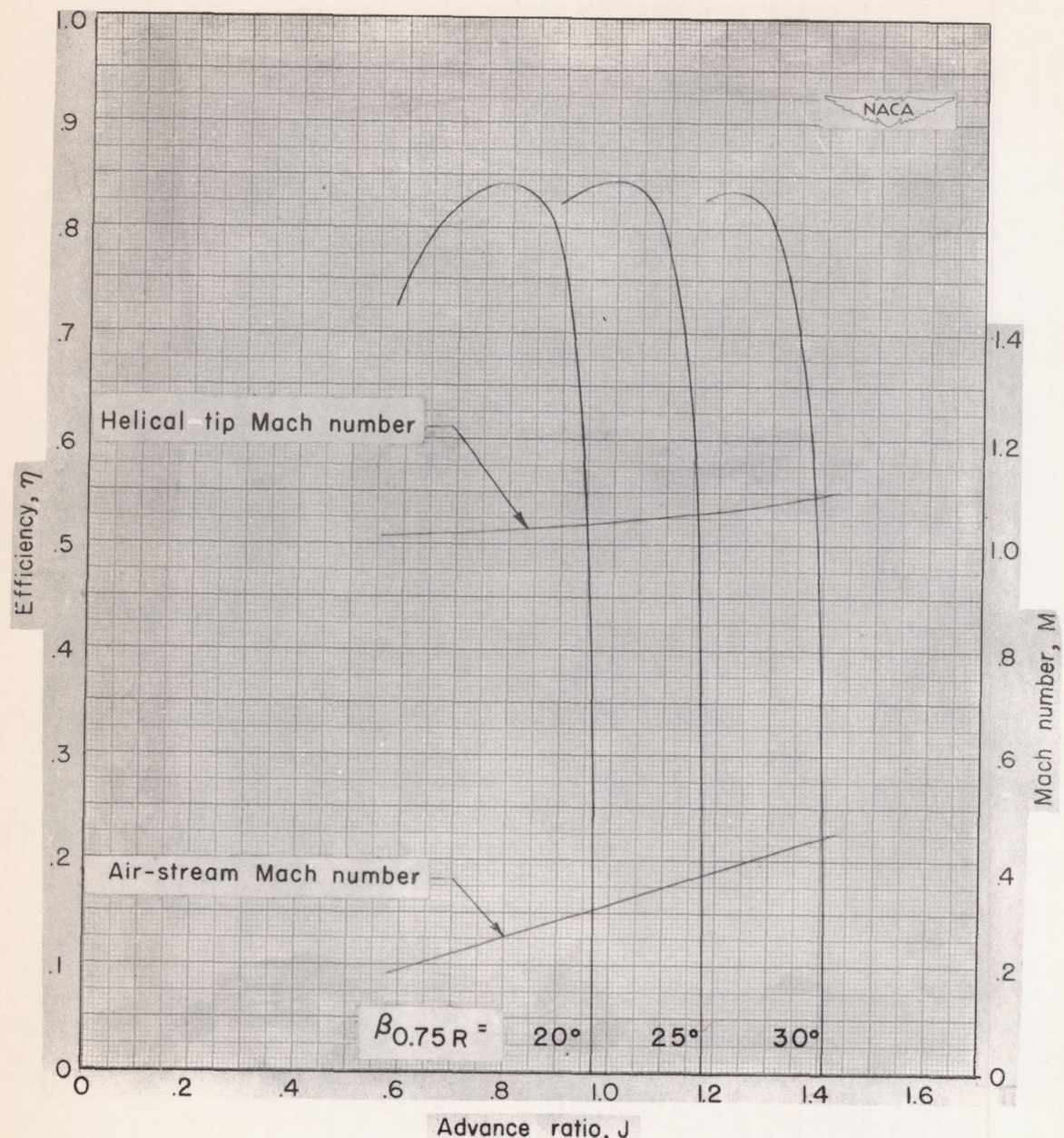
(a) Thrust coefficient.

Figure 9.- Characteristics of two-blade NACA 10-(3)(062)-045 propeller. Rotational speed, 2160 rpm.



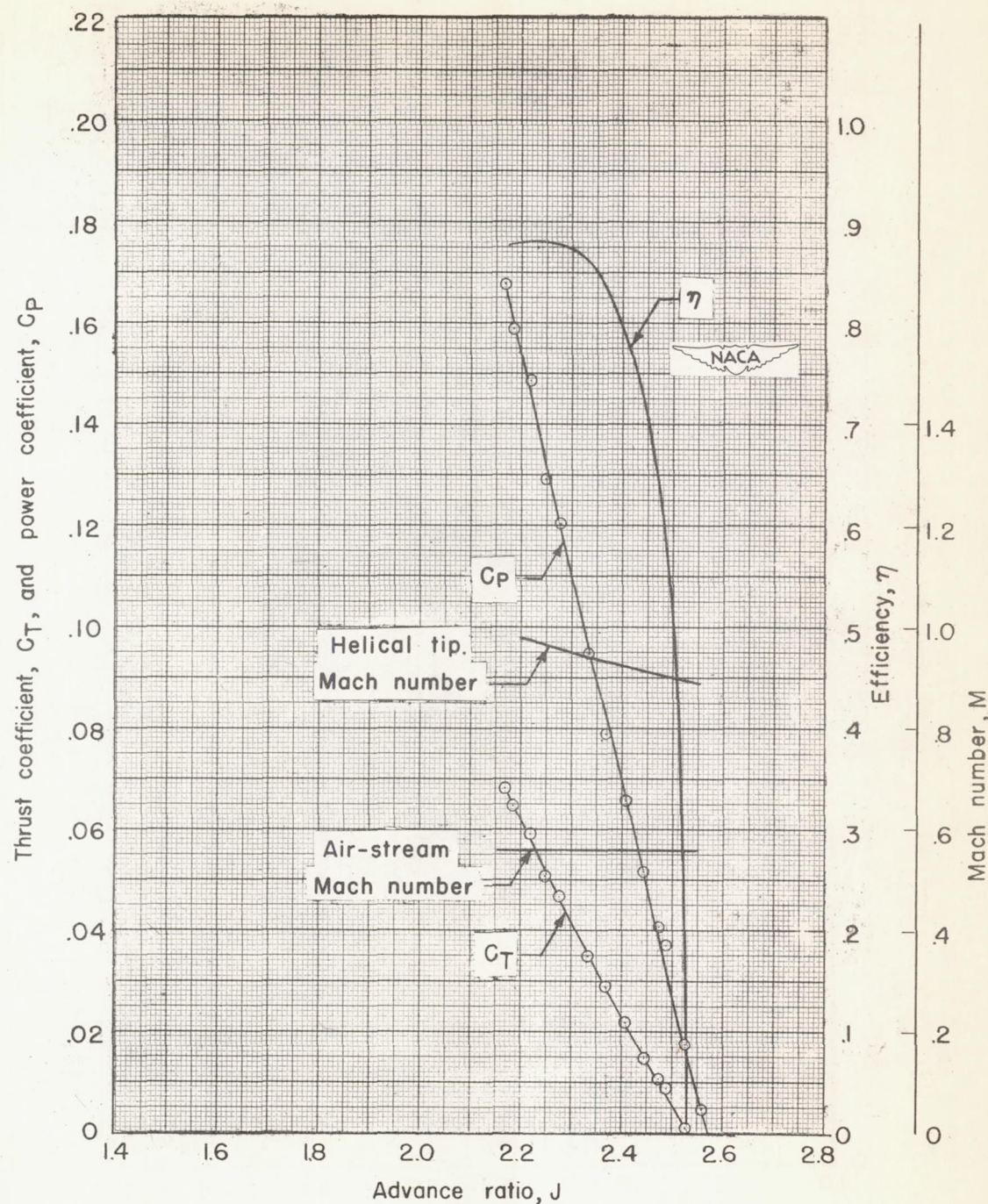
(b) Power coefficient.

Figure 9.- Continued.



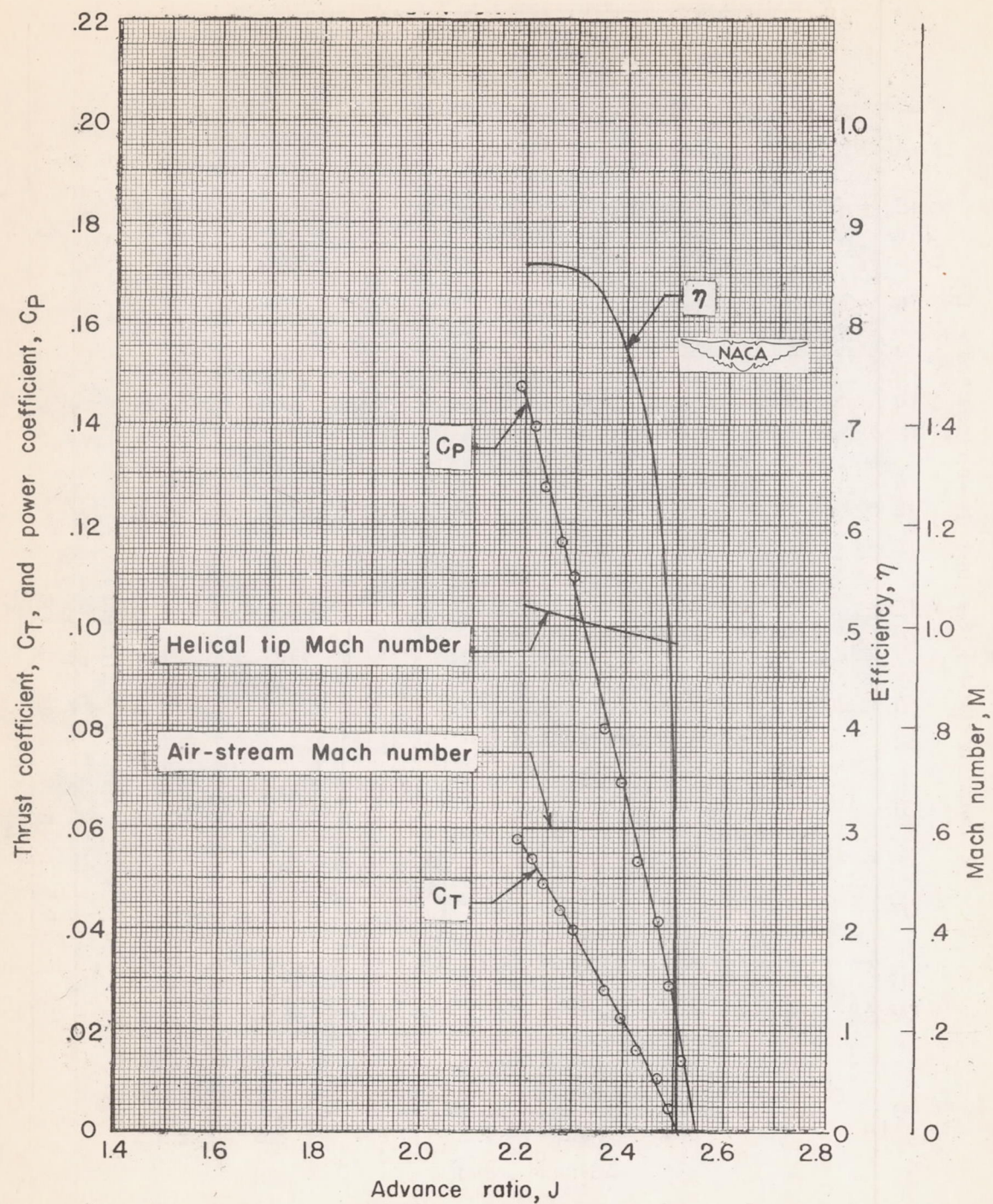
(c) Efficiency.

Figure 9.- Concluded.



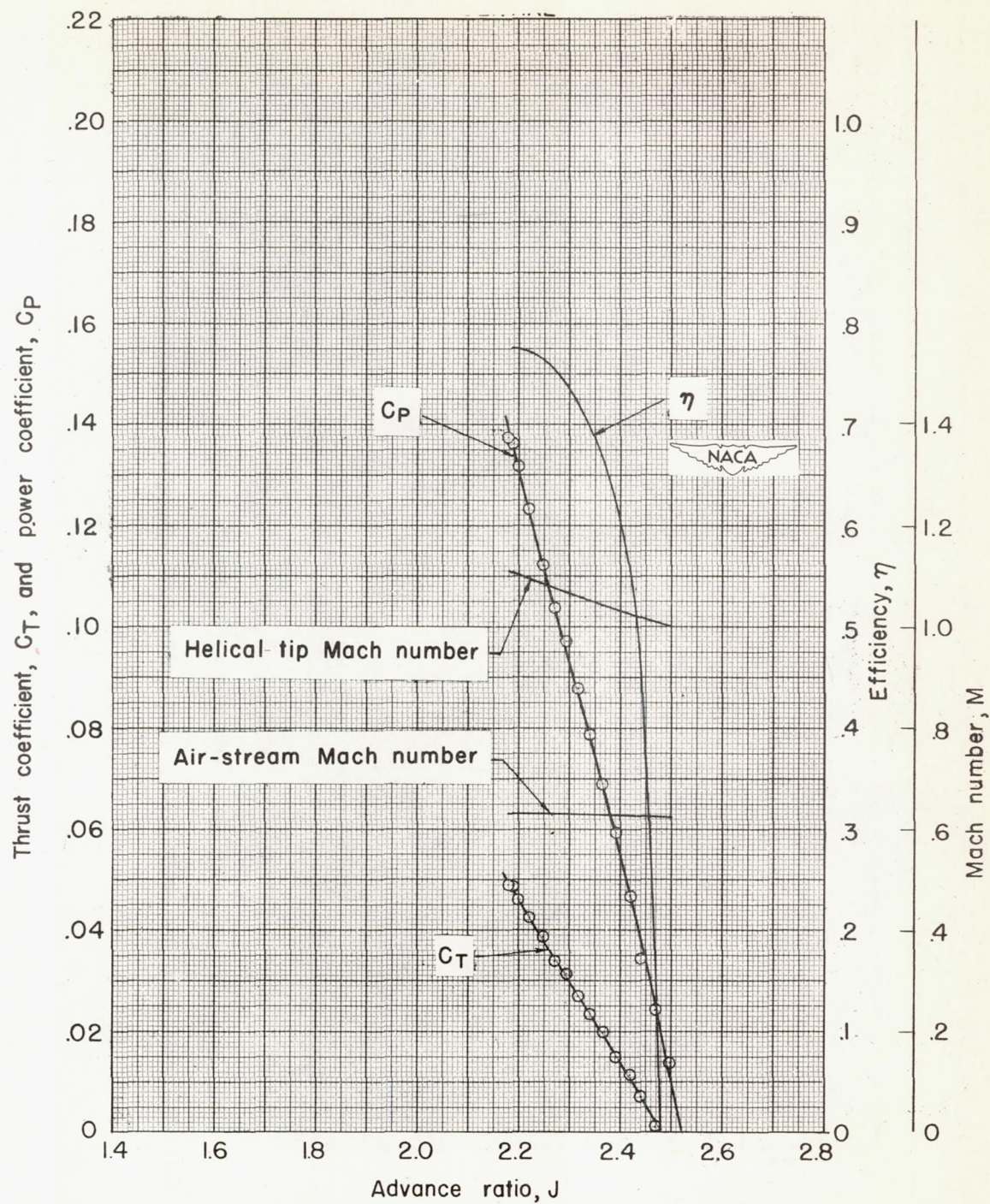
(a) Air-stream Mach number, 0.56.

Figure 10.- Characteristics of two-blade NACA 10-(3)(062)-045 propeller at high forward speeds. $\beta_{0.75R} = 45^\circ$.



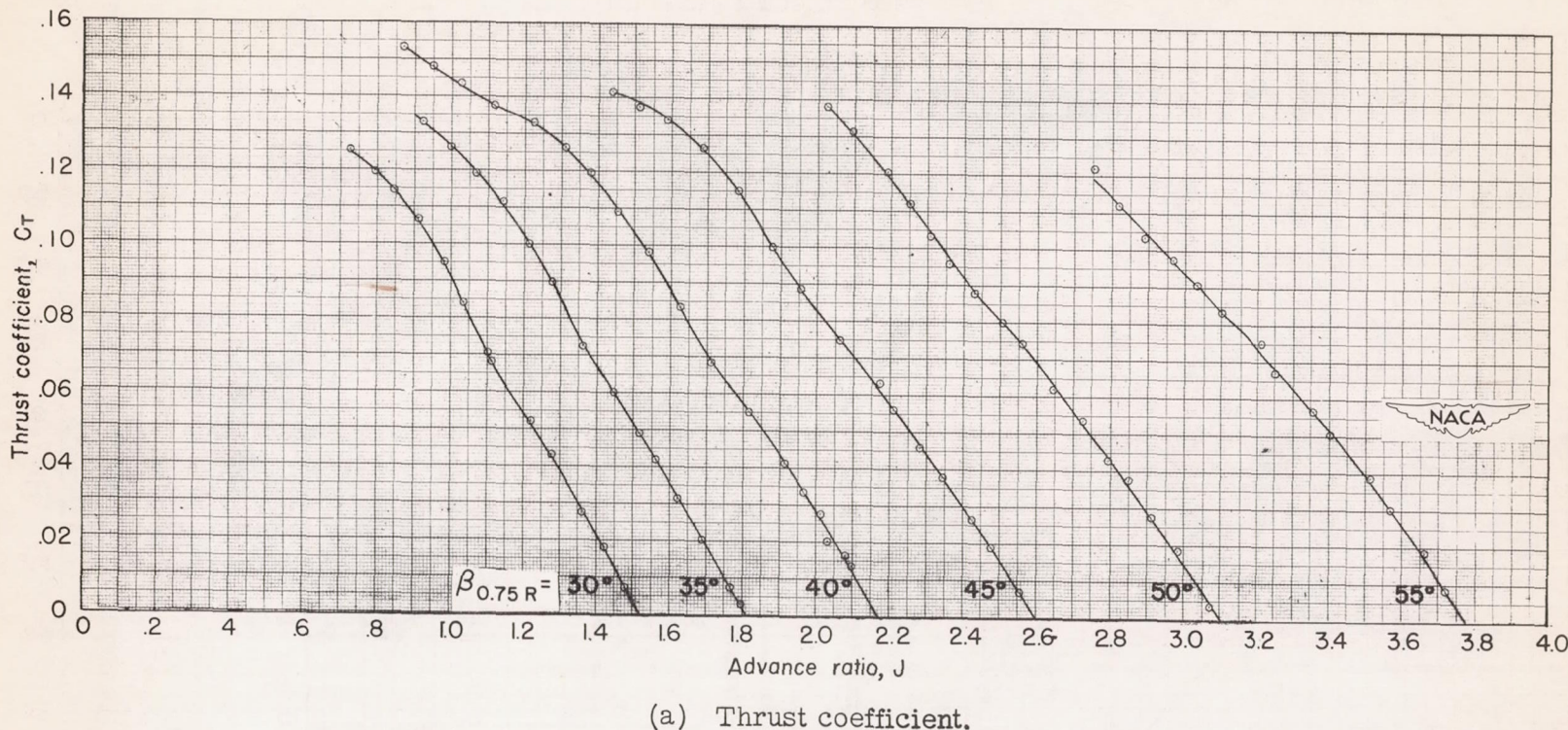
(b) Air-stream Mach number, 0.60.

Figure 10.- Continued.



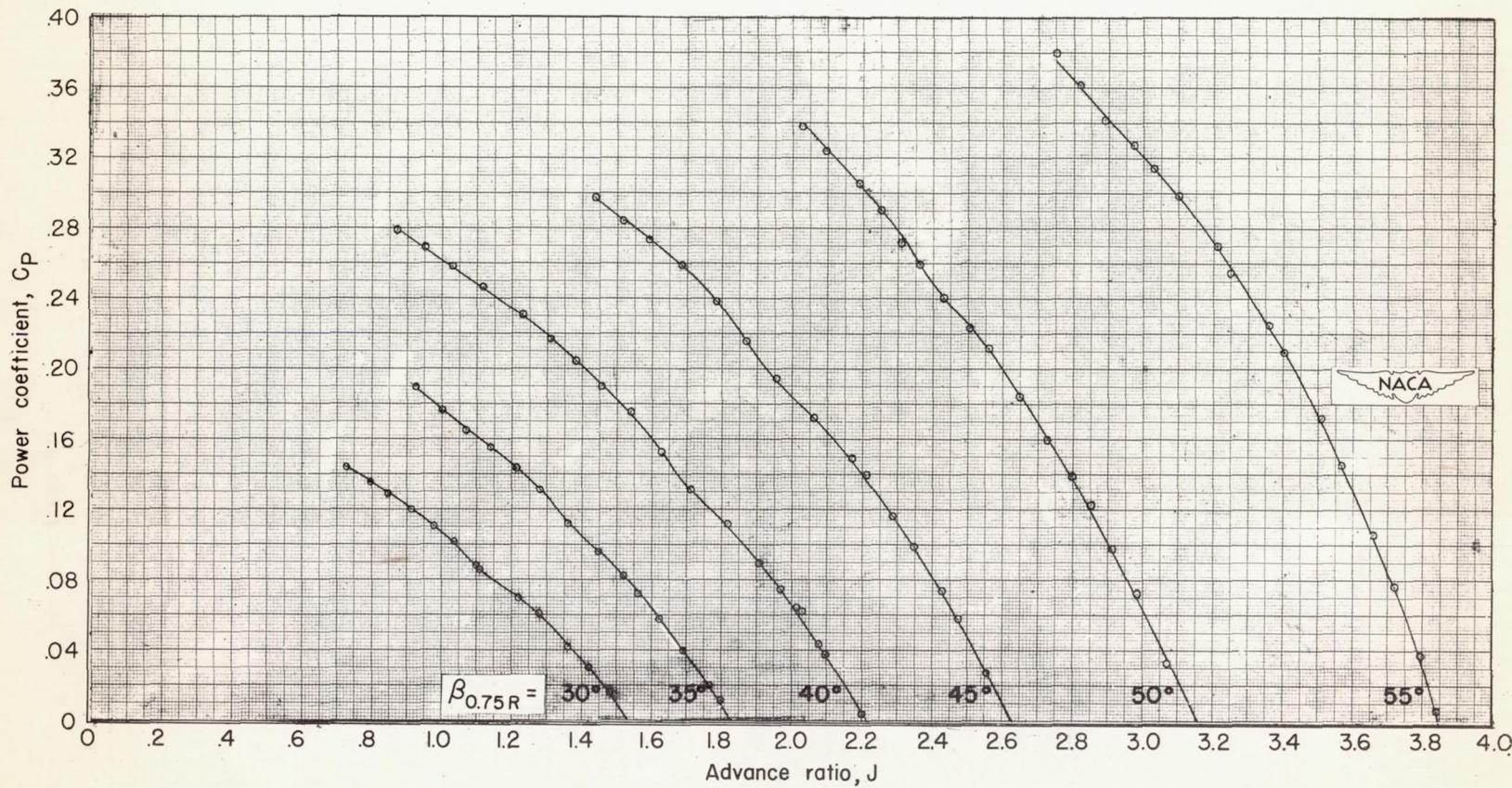
(c) Air-stream Mach number, 0.63.

Figure 10.- Concluded.



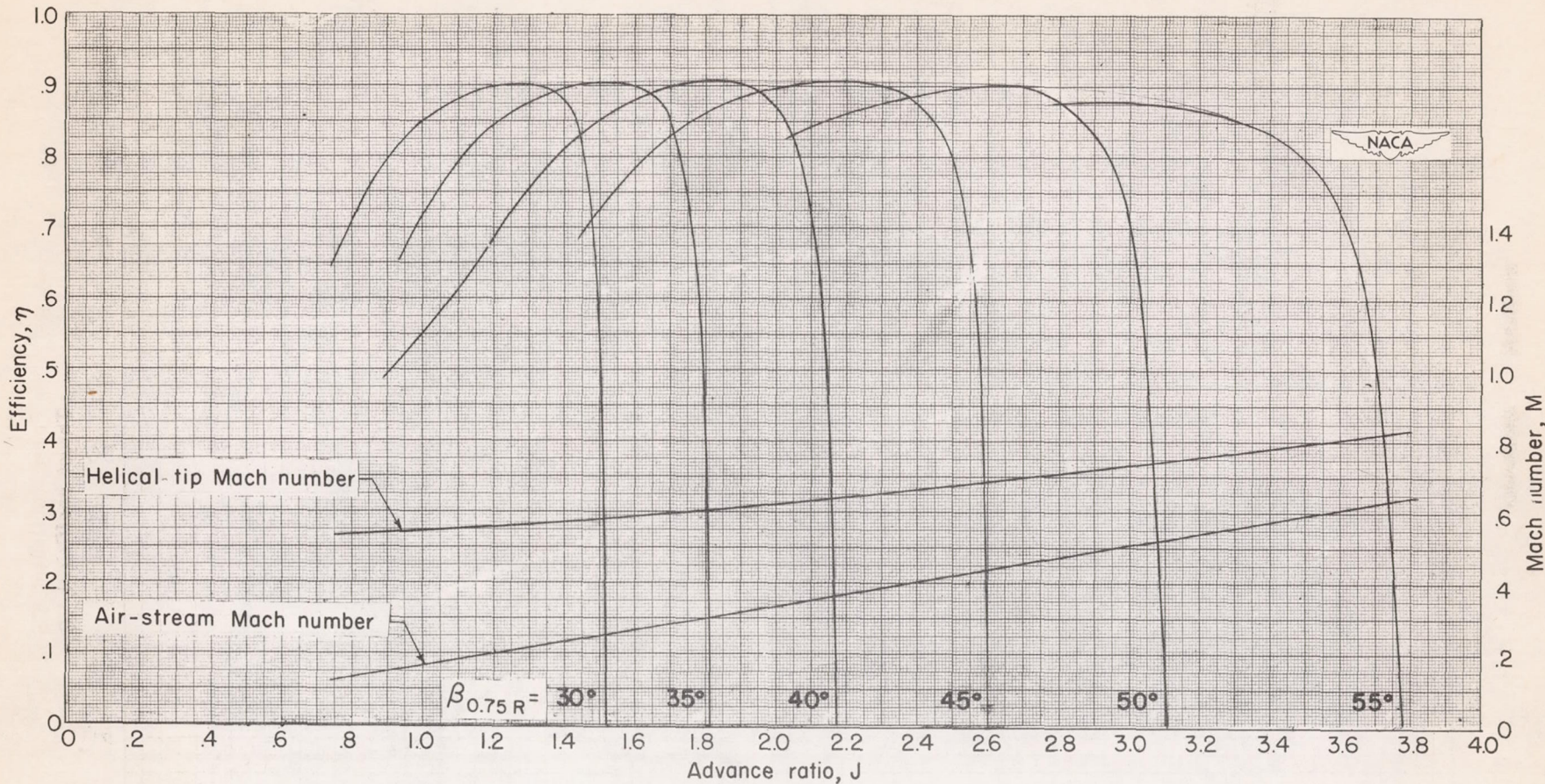
(a) Thrust coefficient.

Figure 11.- Characteristics of two-blade NACA 10-(3)(08)-045 propeller. Rotational speed, 1140 rpm.



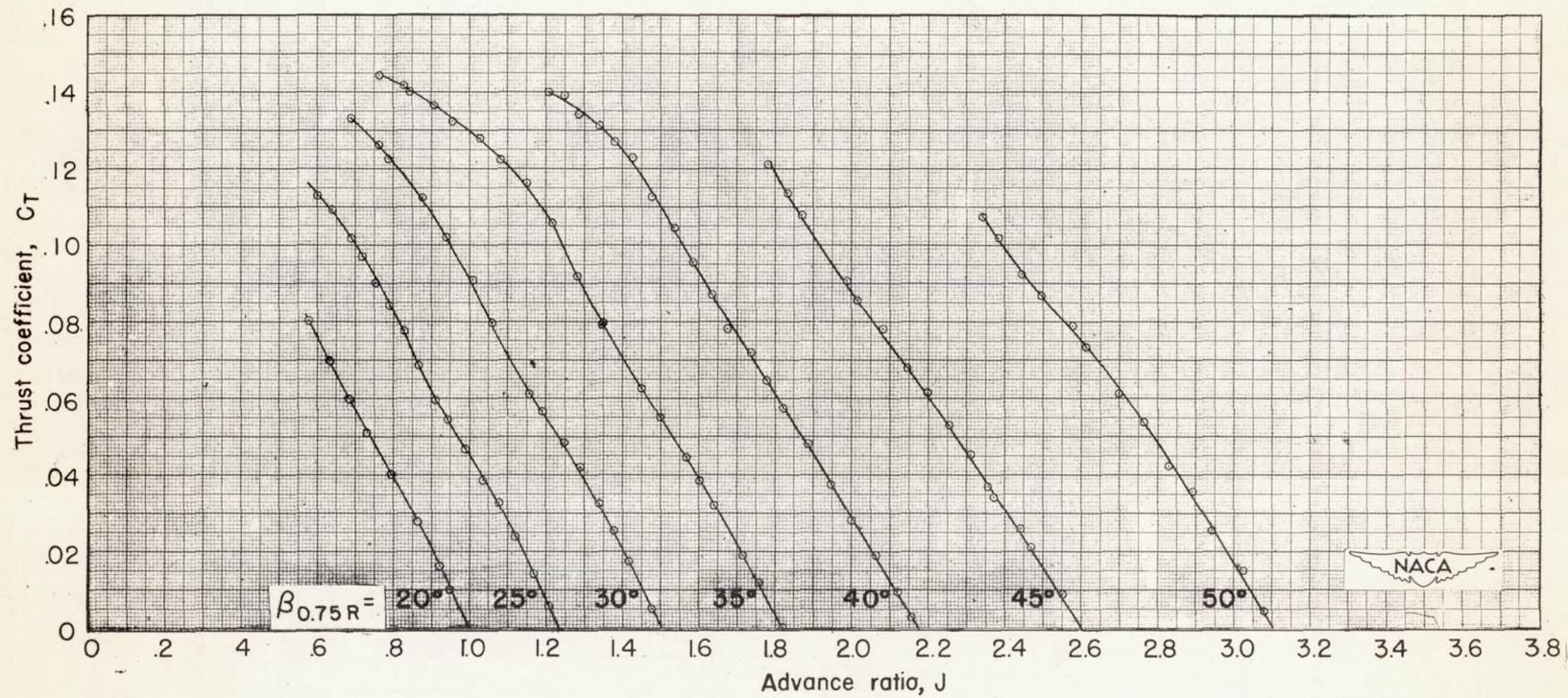
(b) Power coefficient.

Figure 11.- Continued.



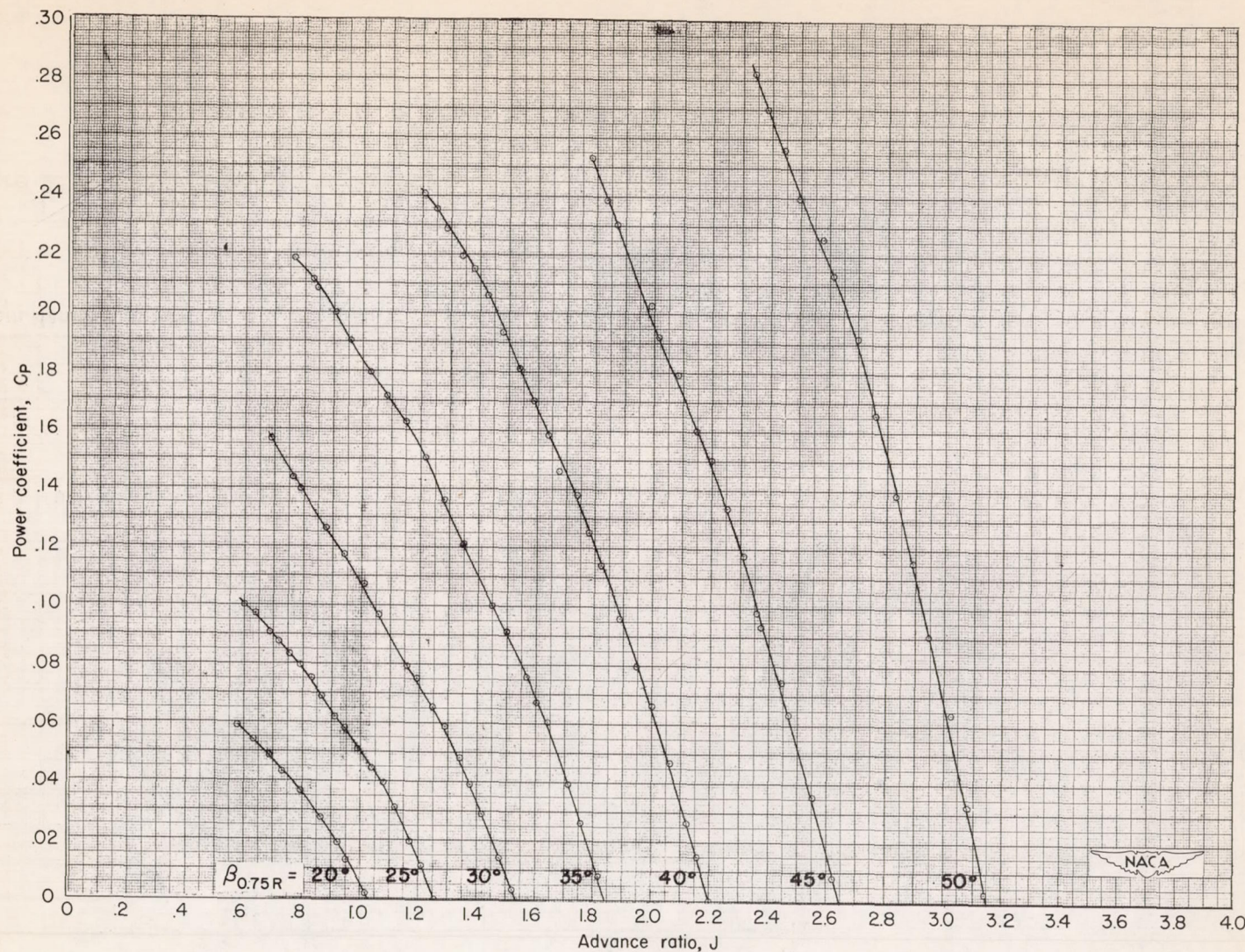
(c) Efficiency.

Figure 11.- Concluded.



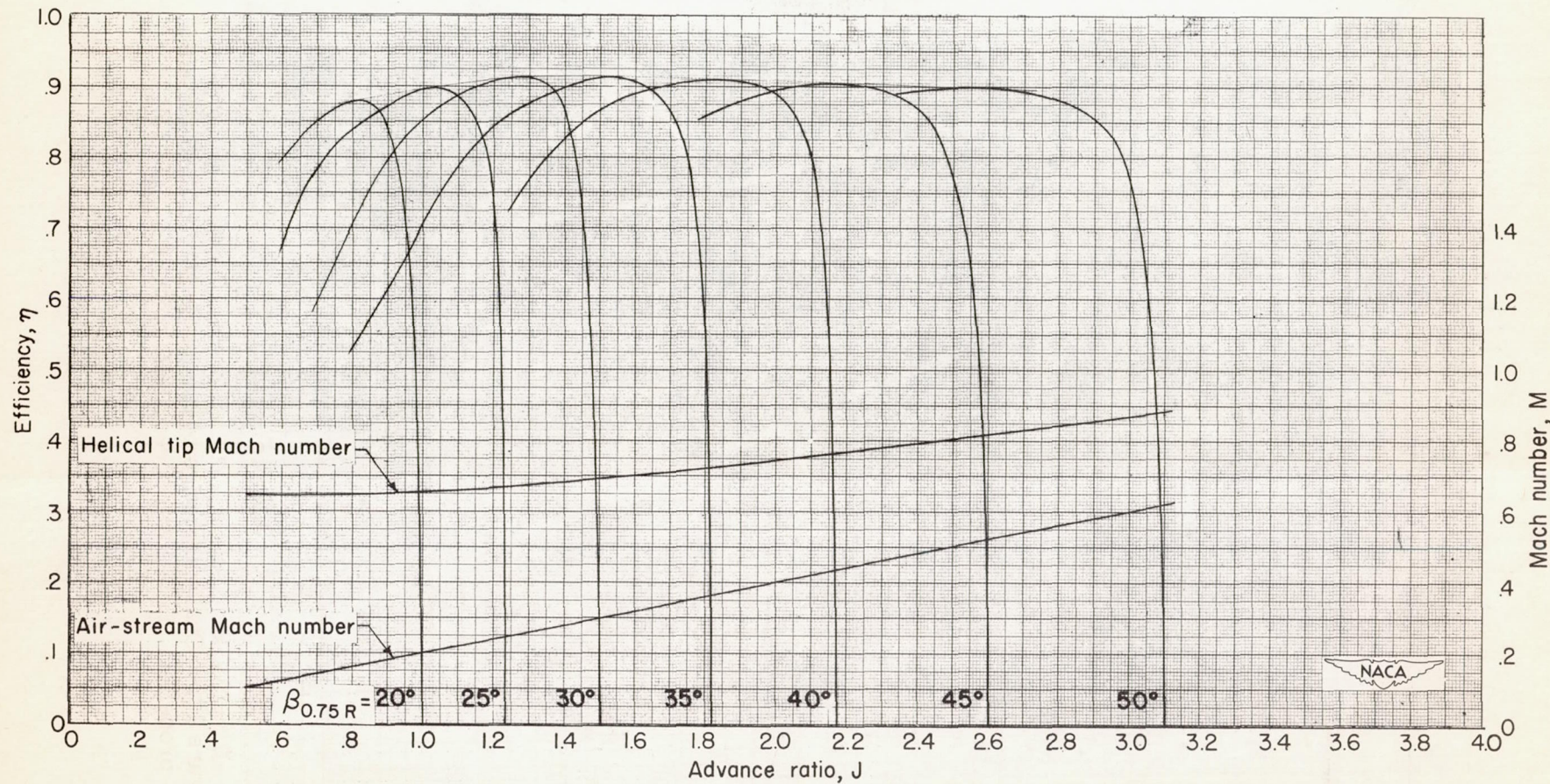
(a) Thrust coefficient.

Figure 12.- Characteristics of two-blade NACA 10-(3)(08)-045 propeller. Rotational speed, 1350 rpm.



(b) Power coefficient.

Figure 12.- Continued.



(c) Efficiency.

Figure 12.- Concluded.

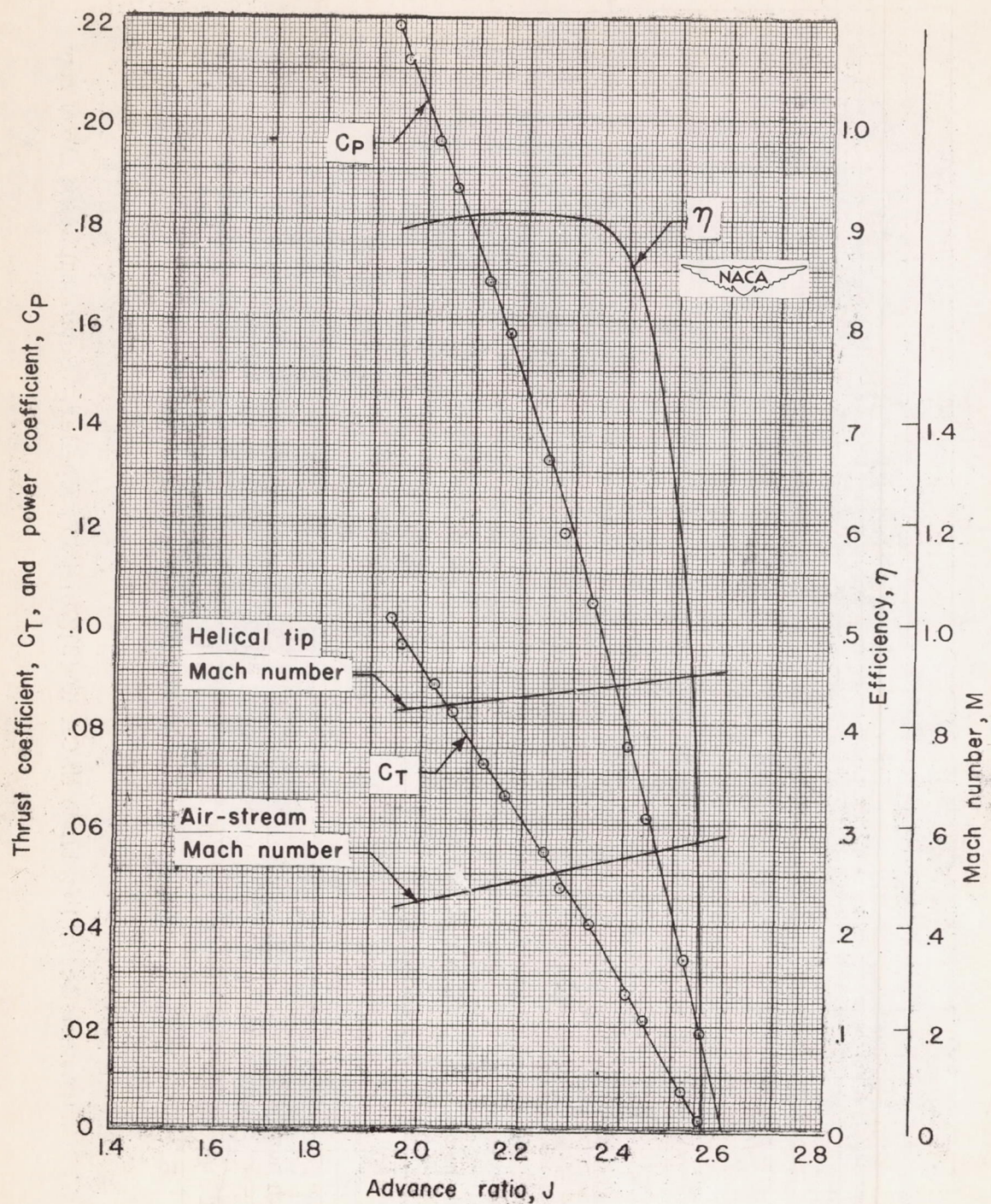
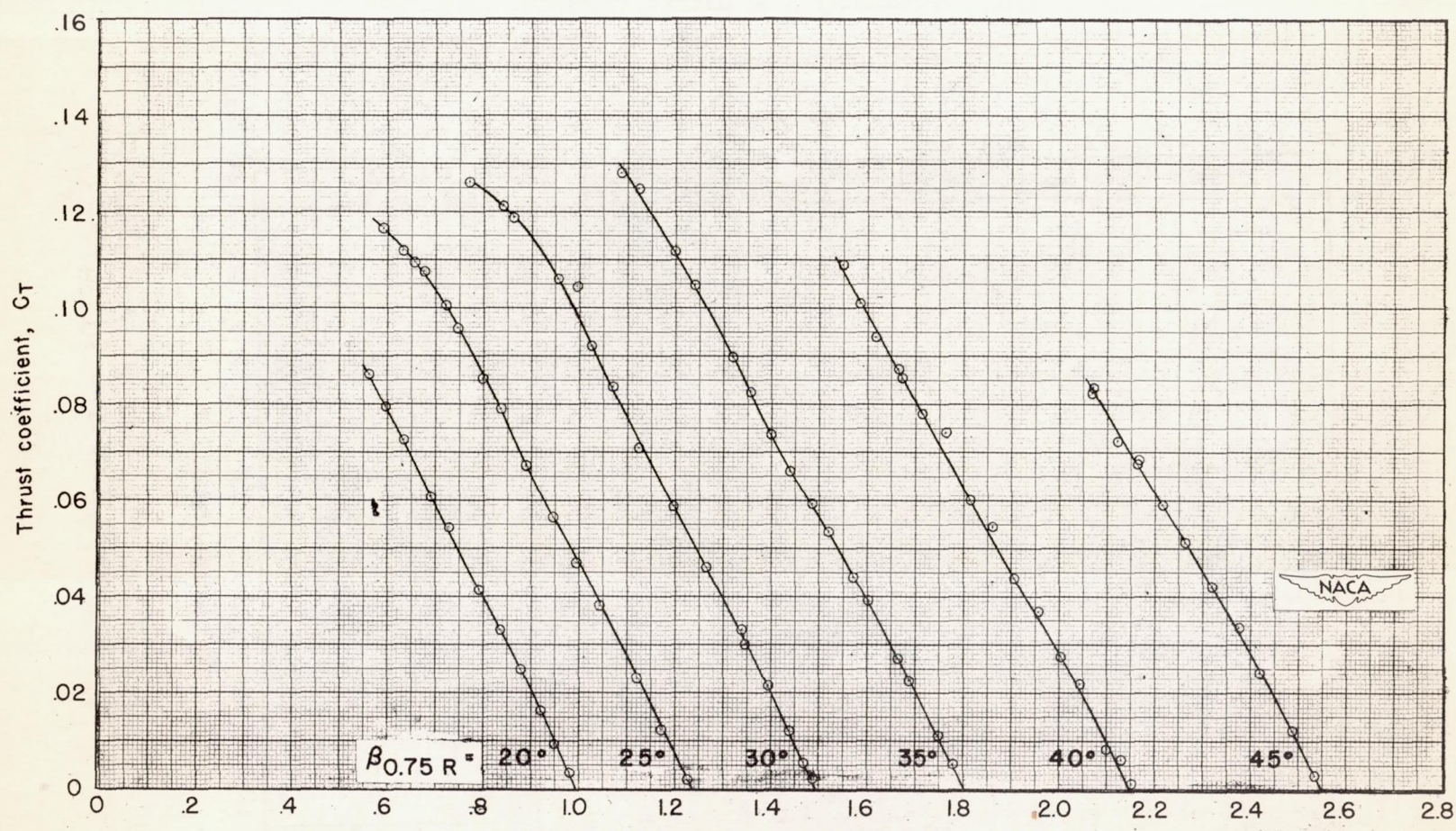
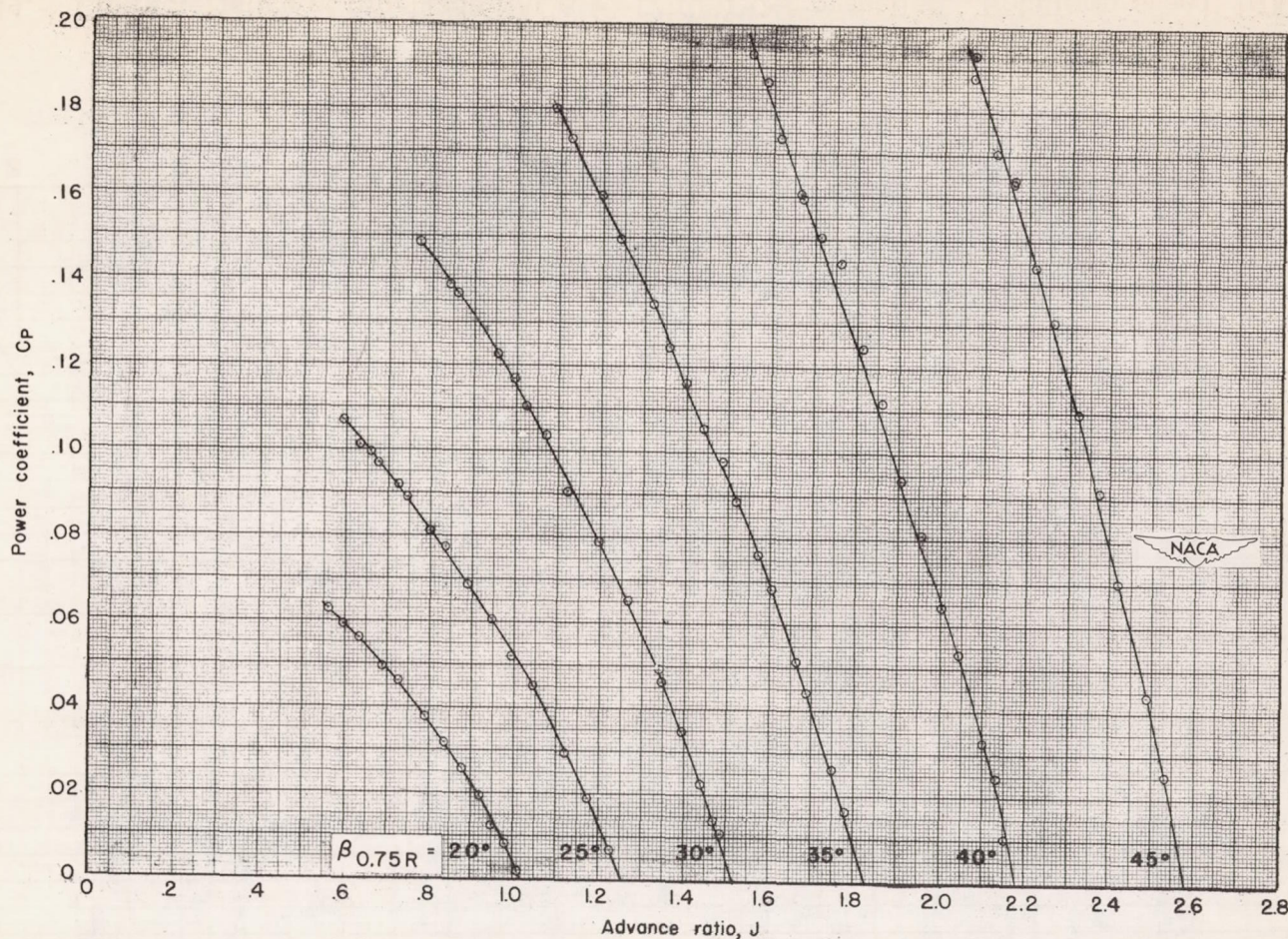


Figure 13.- Characteristics of two-blade NACA 10-(3)(08)-045 propeller. Rotational speed, 1500 rpm; $\beta_{0.75R} = 45^\circ$.



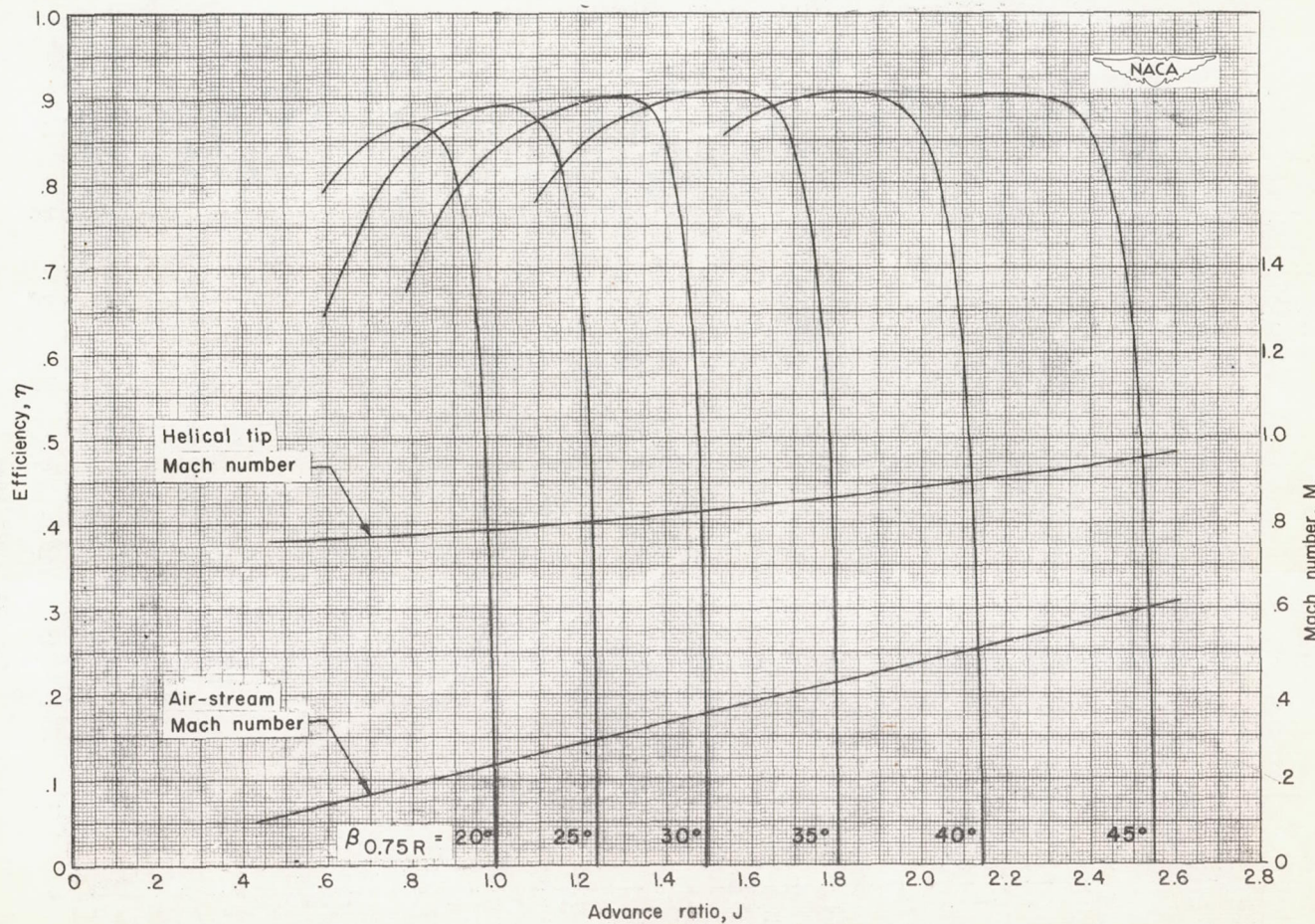
(a) Thrust coefficient.

Figure 14.- Characteristics of two-blade NACA 10-(3)(08)-045 propeller. Rotational speed, 1600 rpm.



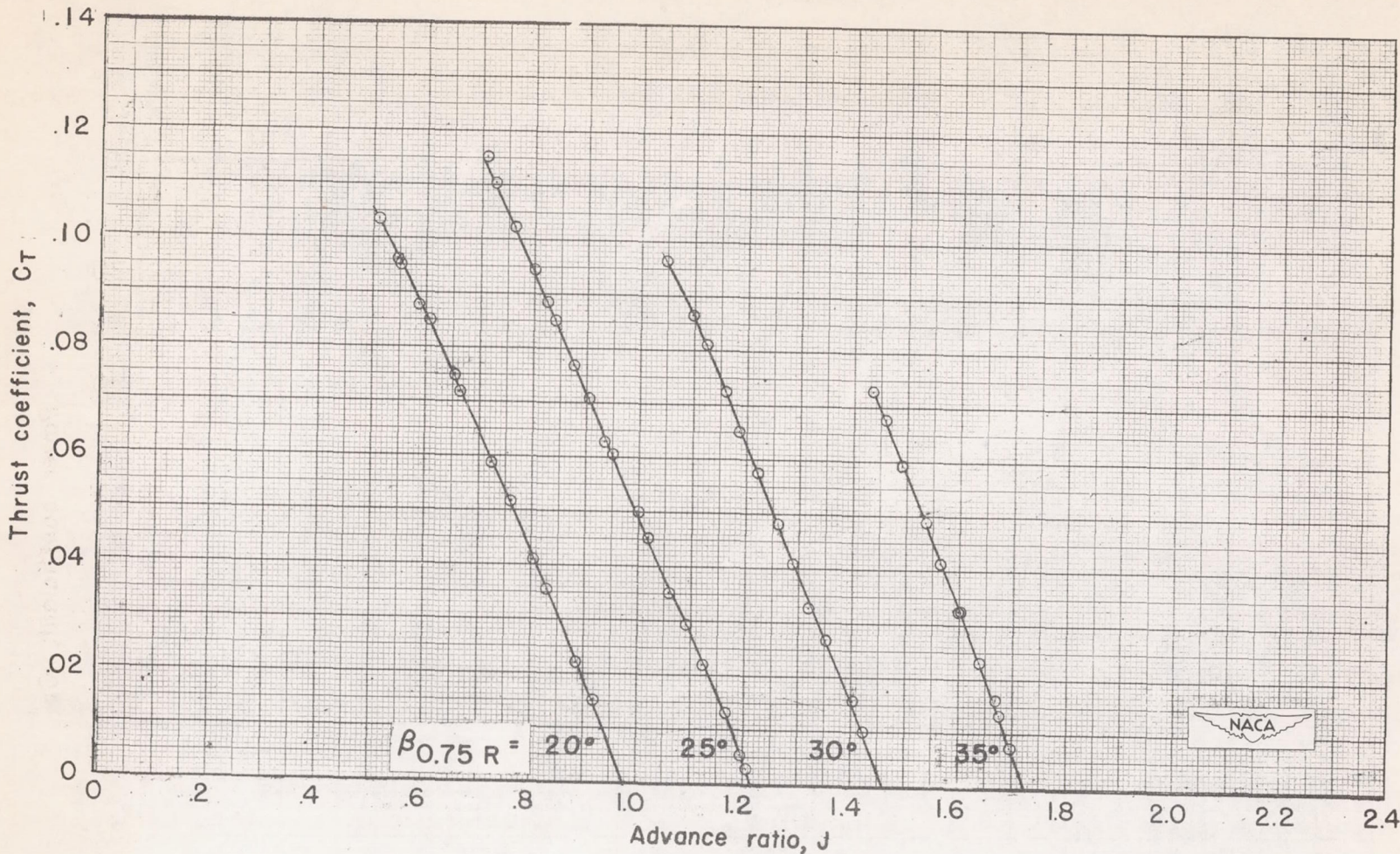
(b) Power coefficient.

Figure 14.- Continued.



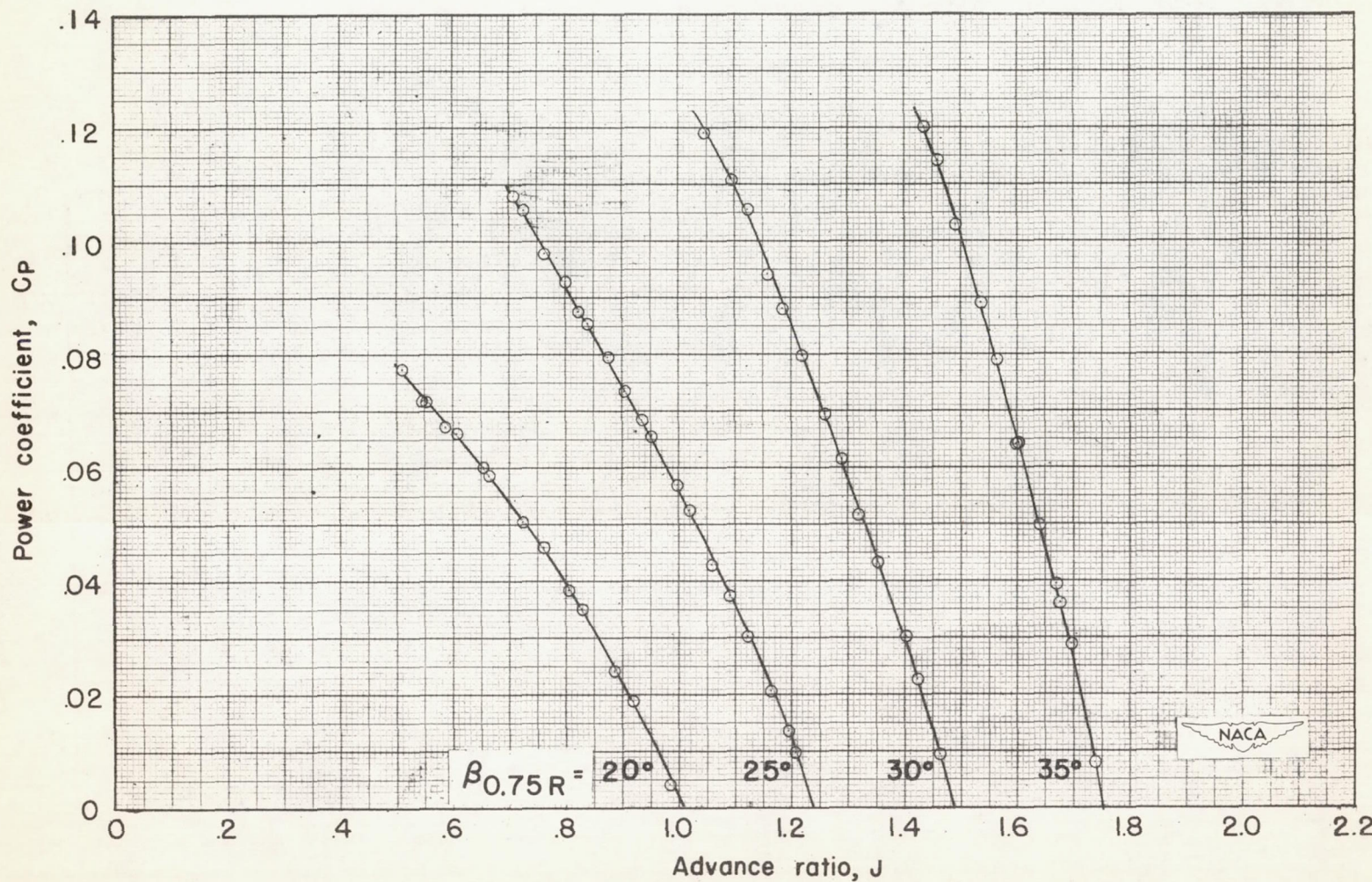
(c) Efficiency.

Figure 14.- Concluded.



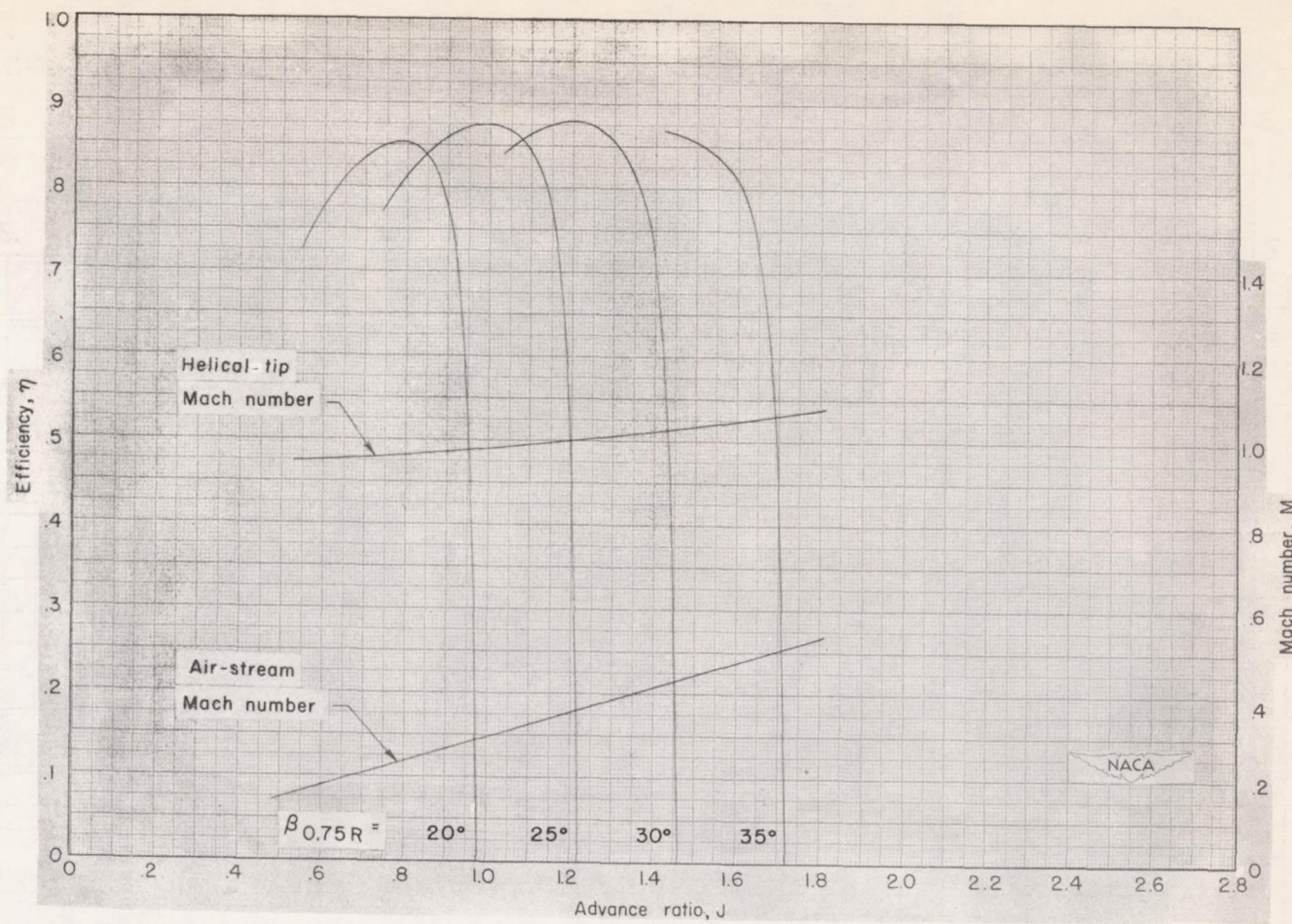
(a) Thrust coefficient.

Figure 15.- Characteristics of two-blade NACA 10-(3)(08)-045 propeller. Rotational speed, 2000 rpm.



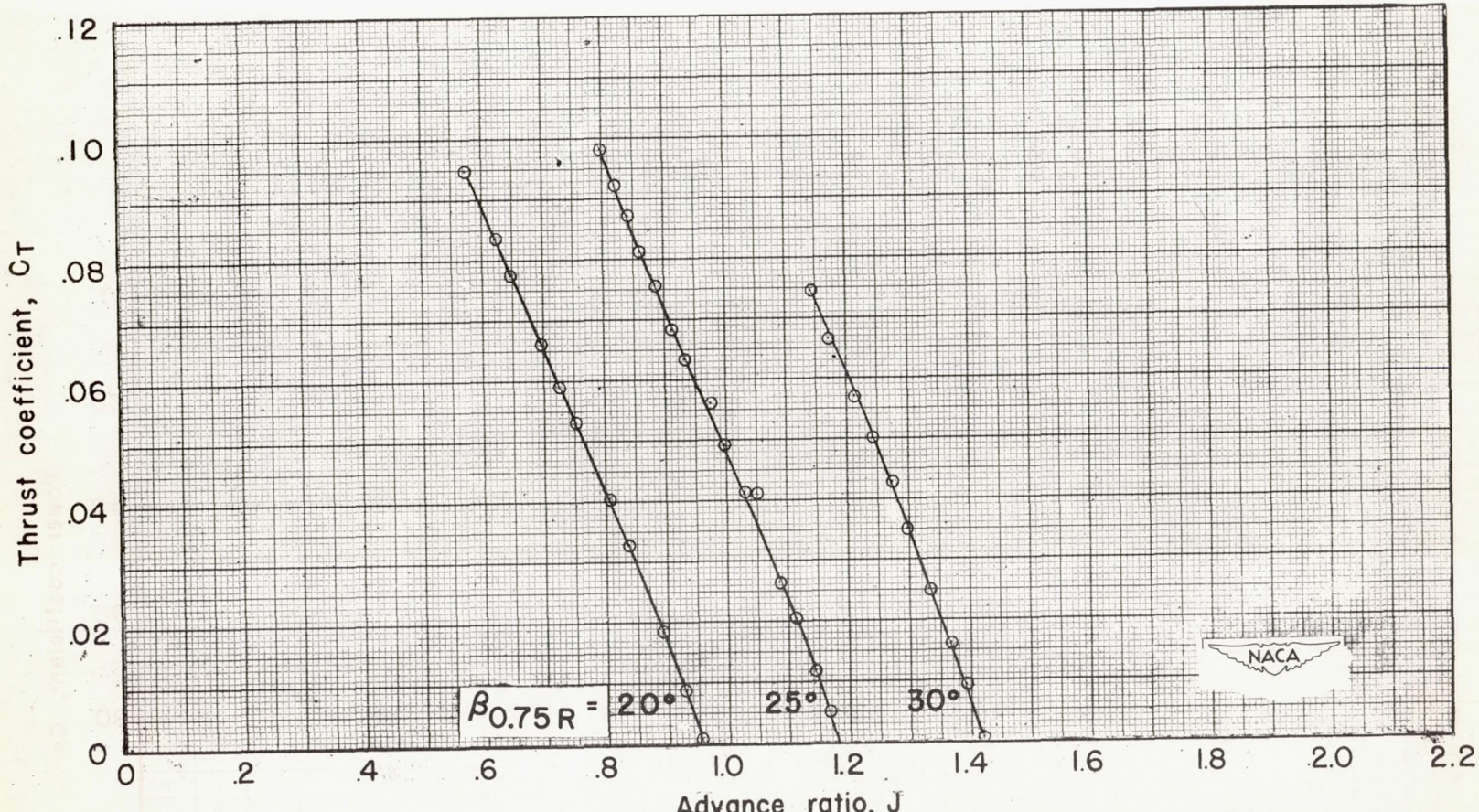
(b) Power coefficient.

Figure 15.- Continued.



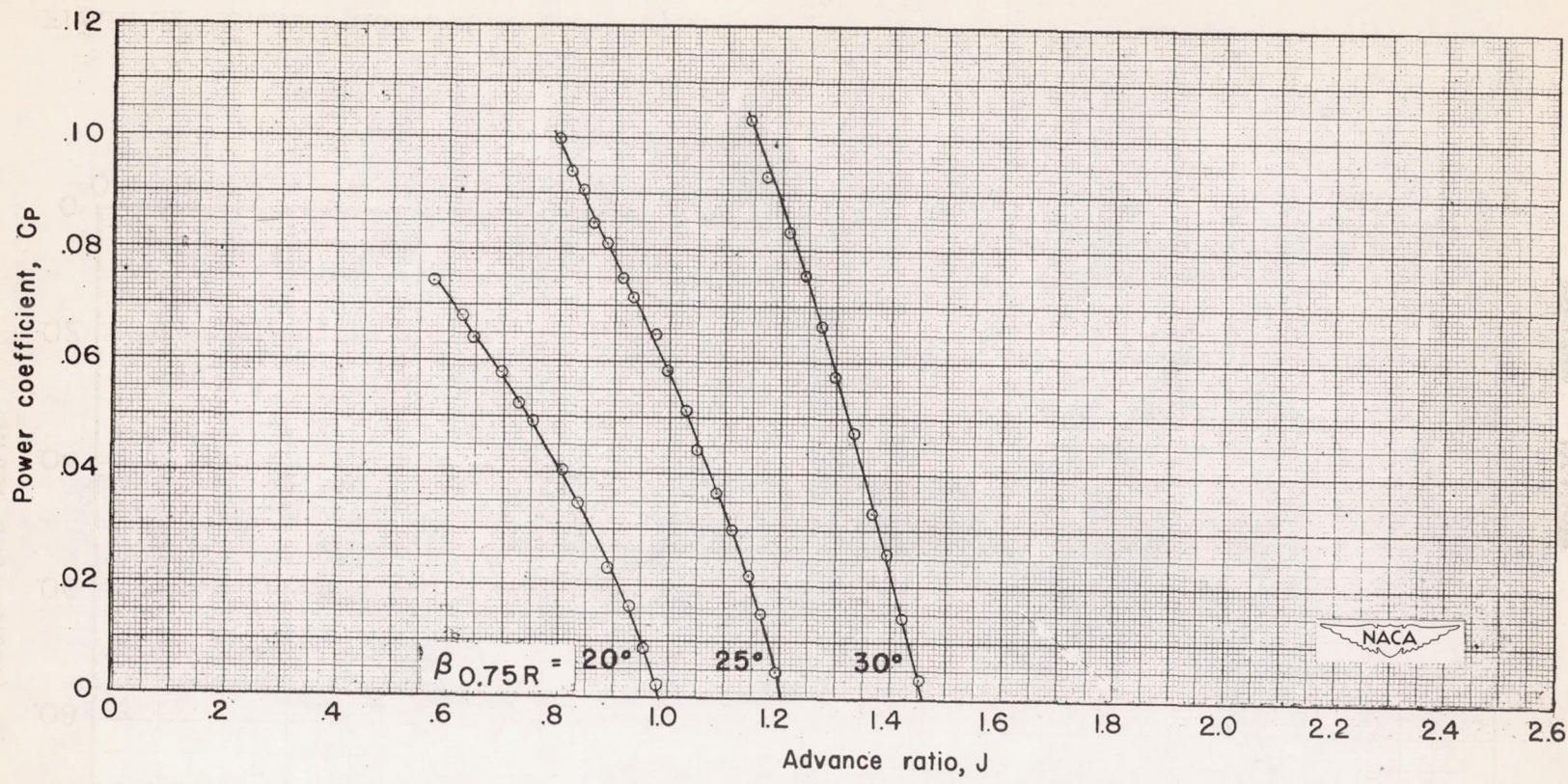
(c) Efficiency.

Figure 15.- Concluded.



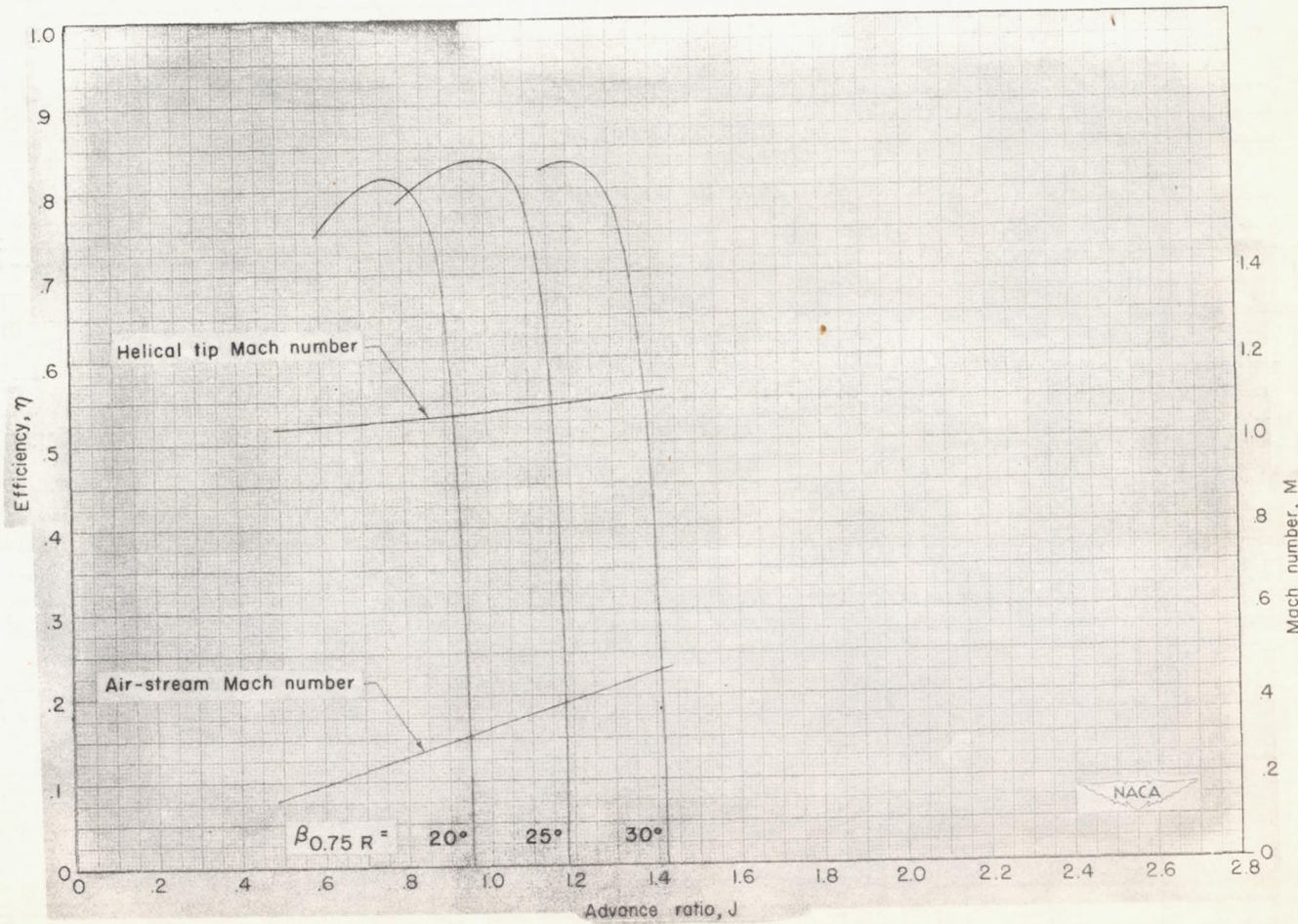
(a) Thrust coefficient.

Figure 16.- Characteristics of two-blade NACA 10-(3)(08)-045 propeller. Rotational speed, 2160 rpm.



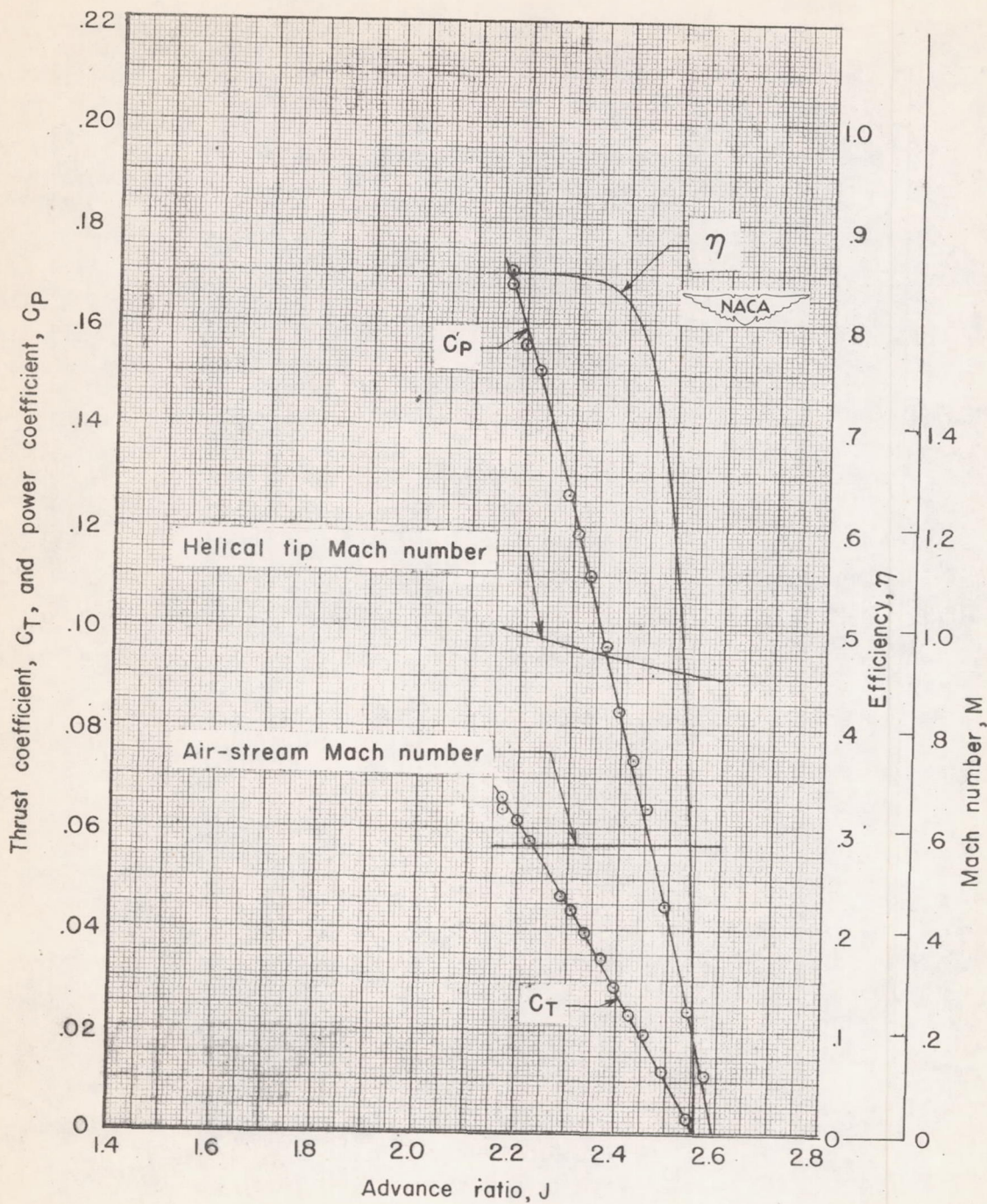
(b) Power coefficient.

Figure 16.- Continued.



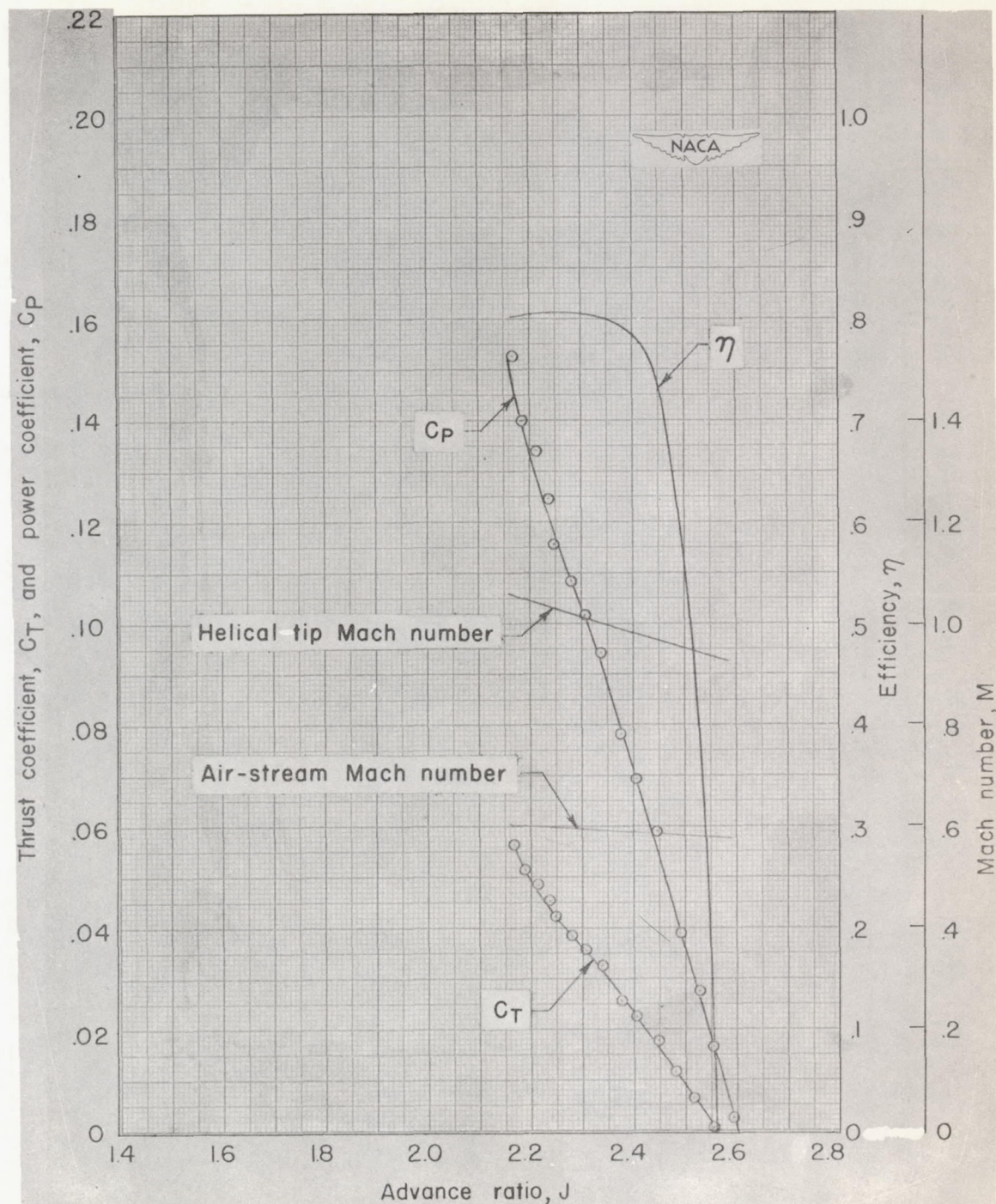
(c) Efficiency.

Figure 16.- Concluded.



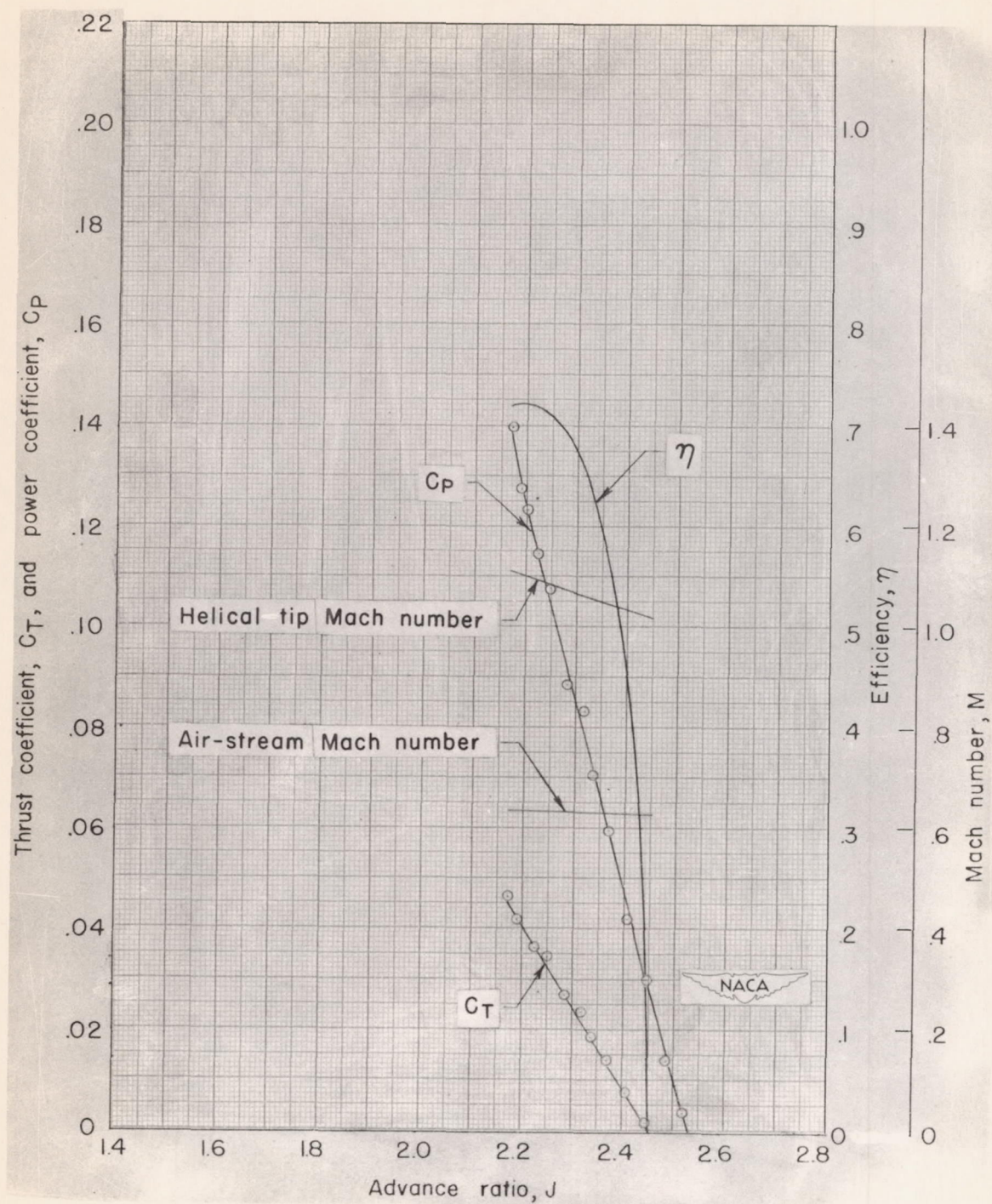
(a) Air-stream Mach number, 0.57.

Figure 17.- Characteristics of two-blade NACA 10-(3)(08)-045 propeller at high forward speeds. $\beta_{0.75R} = 45^\circ$.



(b) Air-stream Mach number, 0.60.

Figure 17.- Continued.



(c) Air-stream Mach number, 0.63.

Figure 17.- Concluded.

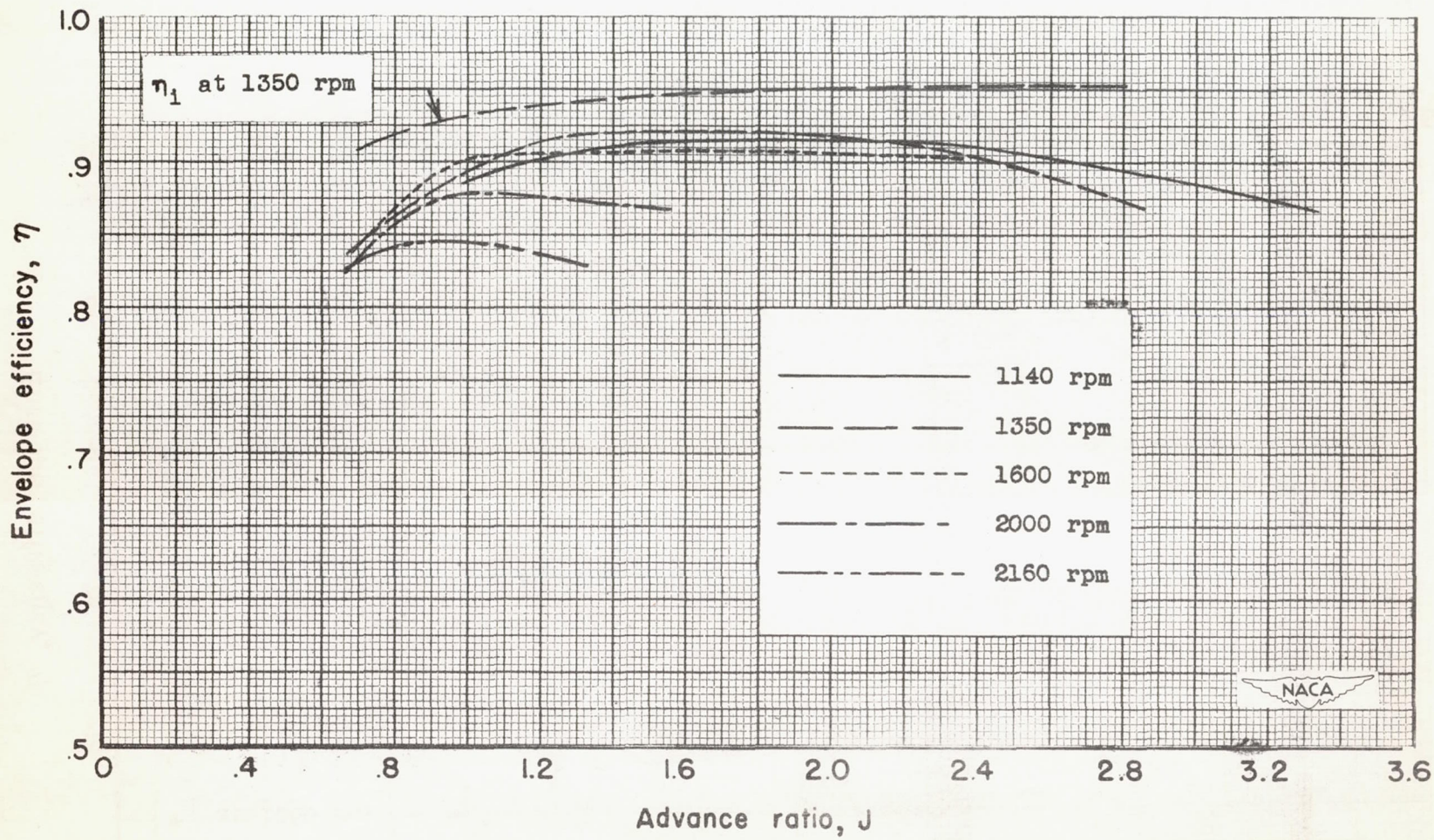


Figure 18.- Envelope efficiency of two-blade NACA 10-(3)(062)-045 propeller at various rotational speeds.

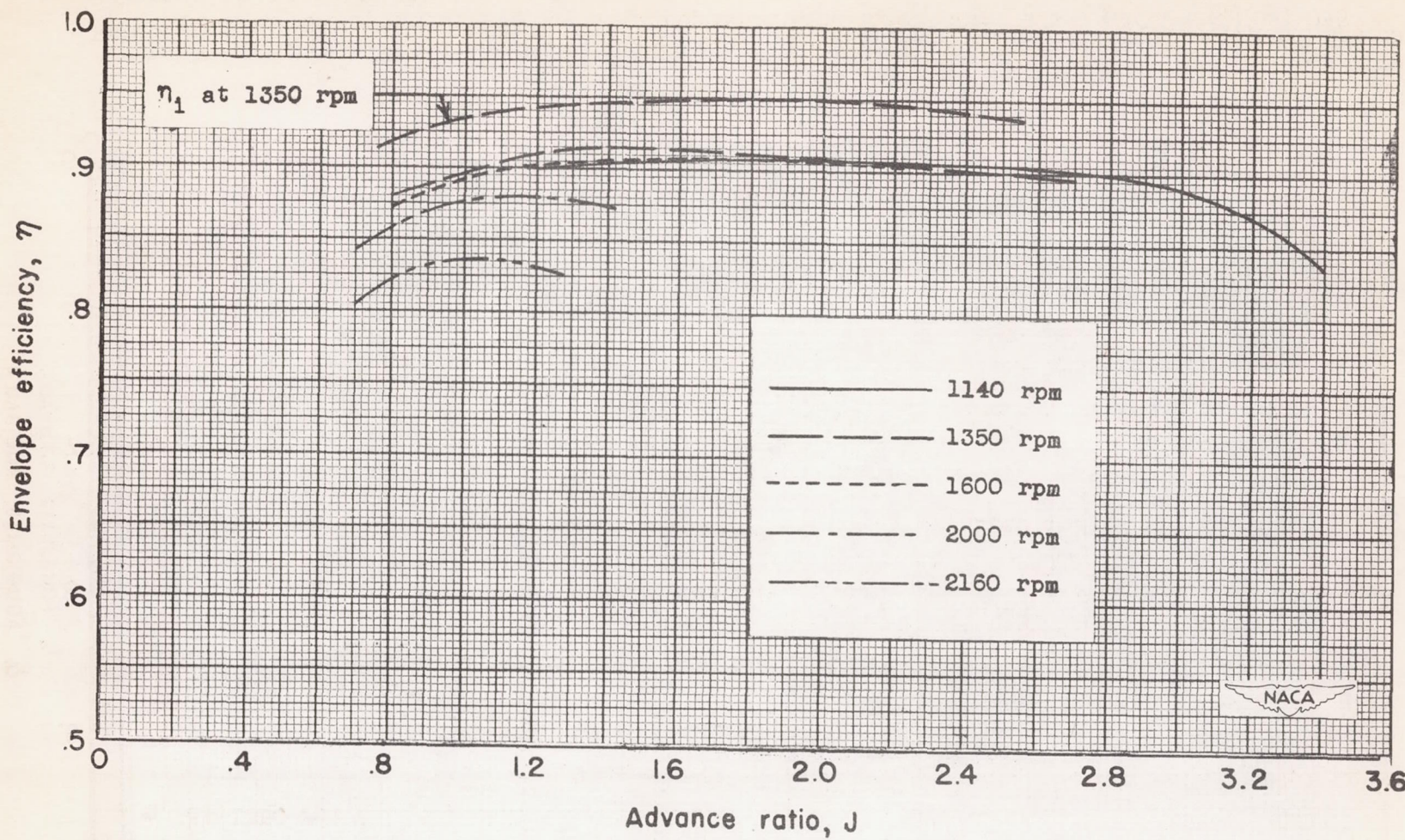


Figure 19.- Envelope efficiency of two-blade NACA 10-(3)(08)-045 propeller at various rotational speeds.

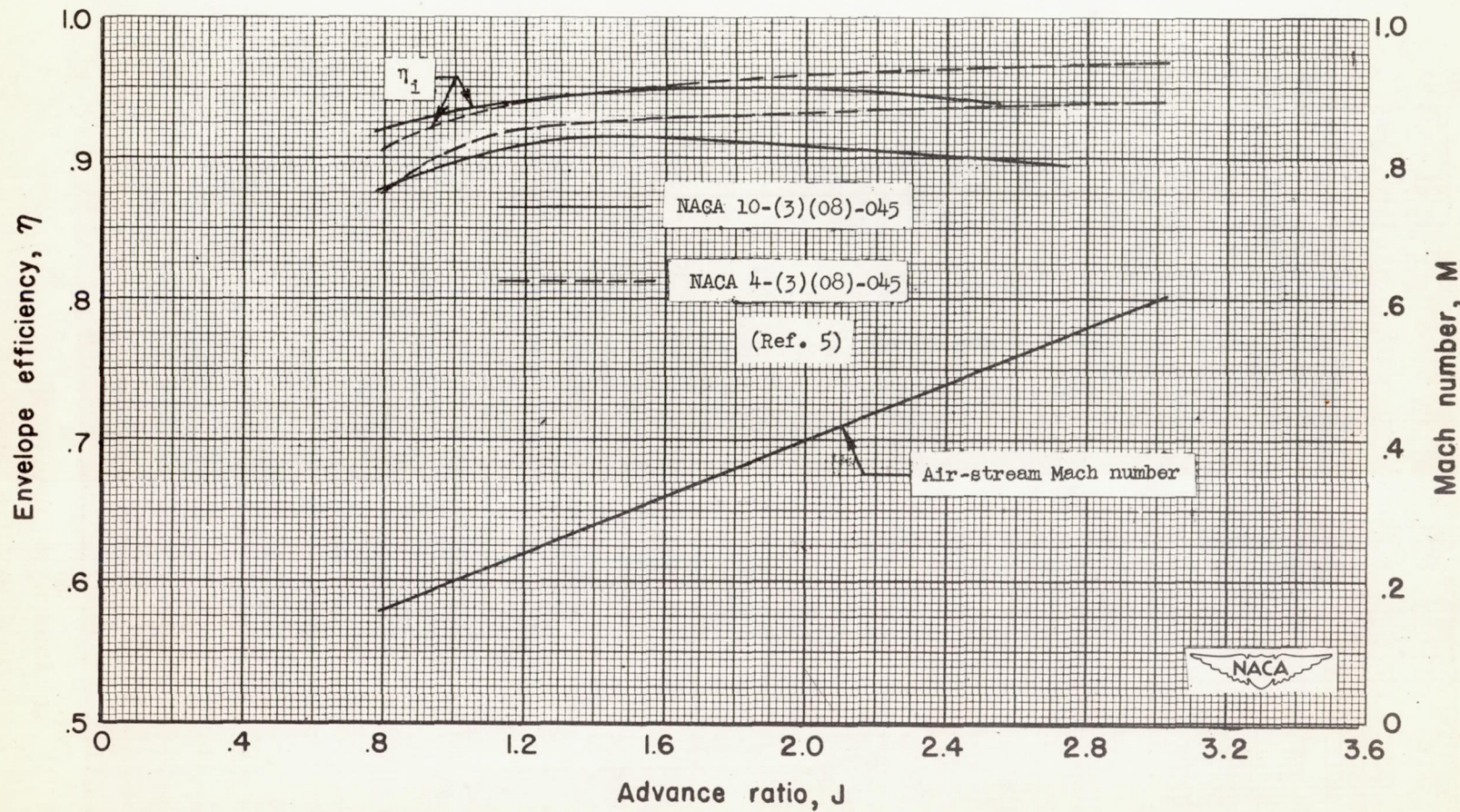


Figure 20.- Comparison of the envelope and the optimum efficiency of a two-blade NACA 10-(3)(08)-045 propeller at 1350 rpm with envelope and the optimum efficiency of a two-blade NACA 4-(3)(08)-045 propeller at corresponding test conditions.

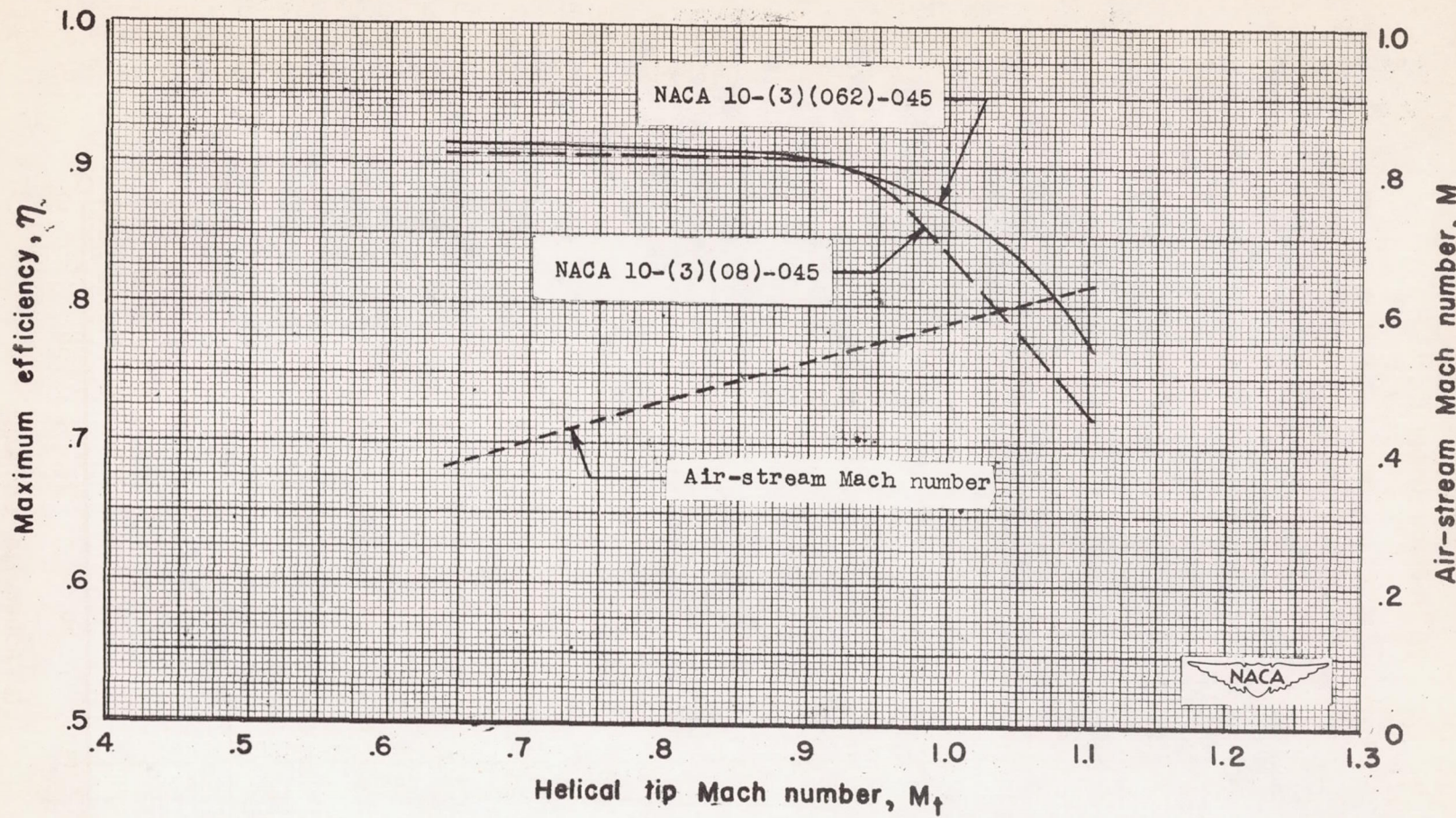


Figure 21.- Effect of compressibility on the maximum efficiency of the two-blade NACA 10-(3)(062)-045 propeller and of the two-blade NACA 10-(3)(08)-045 propeller. $\beta_{0.75R} = 45^\circ$.